DURUM WHEAT METALLOTHIONEIN MUTANTS
and
THEIR BIOPHYSICAL CHARACTERIZATION

by
CEREN SAYGI

Submitted to Graduate School of Engineering and Natural Sciences

in partial fulfillment of

the requirements for the degree of

Master of Science

Sabanci University

June, 2010

DURUM WHEAT METALLOTHIONEIN MUTANTS

and

THEIR BIOPHYSICAL CHARACTERIZATION

APPROVED BY:

Prof. Zehra Sayers …….

(Dissertation Supervisor)

Prof. Yuda Yürüm …….

Prof. Selim Çetiner …….

Doç. Dr. Levent Öztürk …….

Yard. Doç. Dr. Alpay Taralp …….

DATE OF APPROVAL: …….

ABSTRACT

Metallothionein (MT) proteins are characterized as low molecular weight, cysteine (Cys)-rich, metal binding proteins that were discovered more than 50 years ago as Cd-binding proteins present in horse kidney. They have been found in wide range of organisms and their classification was based on the phylogenetic relationships and patterns of distribution of Cys residues along the MT sequences (Binz & Kagi, 2001). They bind a variety of metals with d^{10} electronic configurations through mercaptide bonds with Cys residues (Vasak & Hasler, 2000).

In the present study effects of mutations of Cys residue distributions on the metal-binding properties of a Cd-binding type 1 MT from *Triticum durum* are investigated. For this purpose, modifications were introduced to the cys-motifs of the native durum MT, dMT. Double (G61CG65C) and single mutants (G8C, G12C, G61C, G65C) were produced by site-directed mutagenesis Based on results from earlier work (Bilecen *et al*., 2005) mutants were expressed in *E. coli* as glutathione-S-transferease (GST) fusion proteins. Proteins were purified and characterized by affinity and size exclusion chromatography, SDS- and Native-PAGE, limited trypsinolysis, inductively coupled plasma optical emission spectroscopy (ICP-OES), UV-Vis absorption spectroscopy, circular dichroism spectropolarimetry (CD), dynamic light scattering (DLS), and small-angle X-ray scattering (SAXS).

Expression of the mutants G8C, G12C, G61C and G65C was stable and the proteins were purified for biophysical characterization. Expression of the double mutant G61CG65C, on the other hand, could not be detected in the soluble *E. coli* fractions and efforts to locate it in inclusion bodies also failed. All the over-expressed mutants were purified as homodimers in solution. Protein yield for the mutant preparations ranged between 10 to 15 mg per liter of bacterial culture. The UV-Vis absorption spectra for all the mutants displayed the typical shoulder at 250 nm indicating Cd-binding. The G8C, G12C and G61C mutants had a Cd^{2+} to protein ratio of 3.5±1 which is similar to that observed with native GSTdMT. The G65C, however, showed enhanced Cd binding with a ratio of 4.4 Cd^{2+} per protein, thus binding an additional Cd for each mole of protein compared to native GSTdMT. Proteolytic cleavage results of the G65C indicated that this mutant has more compact structure compared to native

GSTdMT. Shape models obtained from SAXS data of G61C showed that the shape envelope of this mutant is similar to that of the native GSTdMT.

G65C mutant obtained in during these studies offers a possibility for investigation of the Cd-binding mechanisms of MTs and for designing MTs that can be used in applications including biosensors. Future work is needed to understand the basis of enhanced Cd-binding capacity and to determine if this property is preserved when the protein is cleaved from its GST partner.

ÖZET

Metallotioninler (MT'ler) düşük moleküler ağırlıklı olup bünyelerinde bulundurdukları çok sayıdaki sistinler sayesinde metal bağlama özelliğine sahiptirler. MT'ler yaklaşık 50 yıl önce at böbreklerinde kadmiyuma bağlanan proteinler olarak keşfedilmişlerdir. Hemen hemen tüm organizmalarda bulunan MT'ler filogenetik ilişkileri ve sistin gruplarının dağılım düzeni dikkate alınarak sınıflandırılmıstır (Binz & Kagi, 2001). Çeşitli metallere d^{10} elektronik konfigürasyonu ile bağlanırlar (Vasak & Hasler, 2000).

Bu çalışmada *Triticum durum* (makarnalık buğday) tip 1 bitki metallotioninin amino asit dizisindeki sistin gruplarının dağılım düzeninde mutasyonlar yapılmış ve bu mutasyonların proteinin metal bağlama kapasitesi üzeirndeki etkileri araştırılmıştır. Bu amaçla dMT'deki Sistin-X-Sistin motifleri tek ve çift mutasyonlarla değiştirilmiştir. Çift (G61CG65C) ve tek (G8C, G12C, G61C, G65C) mutantlar hedefli mutasyon protokolü ile elde edilmiştir. Önceki çalışmalara dayanılarak (Bilecen ve ark., 2005) mutant proteinler *E.coli*'de GST'ye (glutatyon-S-transferaz) ekli şekilde sentezletilmiştir. Füzyon proteini mutant GSTdMT ve dMT saflaştırılmış, bu proteinlerin yapısal özellikleri ve metal bağlama özellikleri biyofiziksel yöntemlerle incelenmiştir. (Afinite ve moleküler elek kromatografisi, SDS-natif poliakrilamid jel elektroforezi, sınırlı trypsinolisis, atomik emilim spektroskopisi, ultraviyole ve görünür ışık absorpsiyon spektroskopisi, sirküler dikroizm spektrofotometresi, dinamik ışık saçılımı ve solüsyon X-ışını saçılımı ölçümü).

G8C, G12C, G61C ve G65C mutantları sentezletilmiş ve proteinler biyofiziksel karakterizasyon için saflaştırılmıştır. Öte yandan çift mutant G61CG65C çözünebilir *E. coli* fraksiyonlarında da inkluzyon cisimciğinde de tespit edilememiştir. Sentezletilebilen tekli mutantlar homodimer olarak saflaştırılmış ve verimleri 1 litre bakteri kültürü için 10-15 mg olarak tespit edilmiştir. Proteinlerin Cd bağlayıcı özelliğinin göstergesi ultraviyole ve görünür ışık absorpsiyon spektroskopisindeki 250 nm omuzdur. G8C, G12C ve G61C mutant proteinlerin Cd^{2+}/protein oranı 3.5 ± 1'tir aynı yerli GSTdMT gibi. Ancak G65C mutantında protein başına 4.4 Cd^{2+} oranında bağlayıcı özellik tespit edilmiştir. Bu demektir ki G65C mutantı, yerli GSTdMT ile karşılaştırıldığında, bir mol protein için fazladan bir mol Cd^{2+} bağlayıcı bir özellik geliştirmiştir. G65C'nin proteolitik bölünme sonucuna göre bu mutant

yerli GSTdMT'ye göre daha kompakt bir yapıya sahiptir. Solüsyon X-ışını saçılımı ölçümü sonuçlarına göre de G61C ile yerli GSTdMT'nin yapısının benzer olduğunu gösterilmiştir.

Bu çalışmada elde edilen G65C mutantı MT'lerin Cd bağlayıcı mekanizmalarının araştırılması ve MT'lerin biyosensör uygulamalarında kullanılması için bir imkan sunuyor. Geliştirilmiş Cd bağlama kapasitesinin anlaşılması ve bu özelliğin protein GST'den ayrıldıktan sonra korunup korunmadığının araştırılması için çalışmalara devam edilecektir.

To my family for the love

and support they give…

ACKNOWLEDGEMENTS

I would like to thank my supervisor Prof. Zehra Sayers for her wisdom and invaluable guidance from the beginning to the end in the course of my research. She has been a source of inspiration and a guiding light. She taught me how to work hard and how to ski to reduce stress. She was always there to listen and to give advice and taught me how to ask questions and express my ideas. I am sincerely grateful to find the chance of working under her supervision in this project.

I would like to extend my heartiest thanks to Prof. Yuda Yürüm for his rendered assistance and support. The most rewarding experience of my sophomore year was beginning to work in the chemistry lab under the supervision of him.

I'm also so very thankful to the members of the Sayers' lab. Filiz Yeşilirmak for teaching me all the techniques that I used for my thesis, she is very successful and patient scientist. Thanks also to Burcu Kaplan Türköz. She has been a friend and mentor. She helped me for complete the writing of this dissertation as well as understanding the challenging methods that lies behind it. I am sure she will be a successful faculty member in the near future.

A special thanks goes to Mert Aydın, Anıl Aktürk and Erhan Bal. They made the lab a wonderful workplace. They are very smart and warm hearted friends I have ever seen. They continuously joked on me for two years. Whenever I had presentations, I always looked at their faces to calm down. Thank you all for "just being there."

I would like to thank the rest of my thesis committee: Selim Çetiner, Levent Öztürk, Alpay Taralp who gave insightful comments and reviewed my work on a very short notice.

Last, but not least, I am thankful to my beloved parents who taught me the value of education and encourage me to pursue my interests.

TABLE OF CONTENTS

LIST OF FIGURES

LIST OF TABLES

ABBREVIATIONS

bp	Base pair
BSA	Bovine serum albumin
Cd	Cadmium
CD	Circular dichroism
cDNA	Complementary DNA
Co	Cobalt
Cu	Copper
Cys	Cysteine
DLS	Dynamic light scattering
dMT	Durum wheat metallothionein
dNTP	Deoxyribonucleotide triphosphate
DTT	Dithiothreitol
Fe	Iron
GST	Glutathione S-transferase
GSTdMT	Glutathione S-transferase durum wheat metallothionein
G8C	Glutathione S-transferase 8^{th} glycine mutated durum wheat metallothionein
G12C	Glutathione S-transferase 12^{th} glycine mutated durum wheat metallothionein
G61C	Glutathione S-transferase 61^{th} glycine mutated durum wheat metallothionein
G65C	Glutathione S-transferase 65^{th} glycine mutated durum wheat metallothionein
G61CG65C	Glutathione S-transferase 61^{th} and 65^{th} glycine mutated durum wheat metallothionein
HEPES	4-(-2-hydroxyethyl)-1-piperazineethanesulfonicacid

ICP-OES	Inductively coupled plasma optical emission spectroscopy
IPTG	Isopropyl-β-D-thiogalactoside
I(0)	Forward scattering
kDa	Kilodalton
mg	Milligram
ml	Milliliter
μl	Microliter
Nm	Nanometer
PBS	Phosphate buffered saline
PCR	Polymerase chain reaction
PMSF	Phenylmethanesulphonylfluoride
PMW	Unstained protein molecular weight marker
P(r)	Distance distribution function
Rg	Radius of gyration
SAXS	Small angle X-Ray scattering
α	Alpha
β	Beta
Zn	Zinc

1. INTRODUCTION

Metallothioneins (MTs) are a family of cysteine (Cys)-rich low molecular weight proteins. They are found throughout the animal kingdom and are also found in higher plants, eukaryotic microorganisms, and in some prokaryotes. MTs have high affinity for soft d^{10} metal ions due to their high amount of polarizable cysteine thiolate ligands. Naturally occurring MTs are generally isolated with Zn(II), Cd(II) and Cu(II). However, Ag(I), Au(I), Bi(III), Co(II), Fe(II), Hg(II), Ni(II), Pt(II), and Tc(IV)O are metal ions that bind to the protein in vitro (Vasak & Romero-Isart, 2002).

MTs were classified by different methods according to their primary structure. One of the classifications, performed by Binz and Kagi (2001), was based on phylogenetic relationships and the patterns of distribution of Cys residues along the MT sequences (Binz & Kagi, 2001). This analysis resulted in a classification of 15 families and plant MTs are the last family. They have been further classified by Cobbet and Goldsbrough (Cobbett & Goldsbrough, 2002) into 4 types as well.

Most protein-metal binding studies are carried out on mammalian proteins and little is known about the structural features the plant MTs. A novel MT gene (*dmt*) in *Triticum durum* was identified and cloned for overexpression in *E.coli* (Bilecen *et al.*, 2005). It is a type-1 plant MT and displays three sequence domains: metal binding N terminus (β domain, 1-19th residues) and C terminus (α domain, 61-75th residues) and a long hinge region (20-60th residues). Cys residues are clustered equally in N and C termini with a "Cys-X-Cys" motif and the hinge region possess no Cys residues. dMT was overexpressed in *E.coli* as a GST (glutathione-S-transferase) fusion protein (GSTdMT). Both GSTdMT and dMT cleaved from GST were purified and characterized by biochemical and biophysical methods. It was shown that GSTdMT binds 3.5±1 moles of Cd per one mole of protein and has a high tendency to form stable oligomeric structures (Yesilirmak, 2008).

The work presented in this thesis concerns the expression, purification, and biochemical and biophysical characterization of mutant GSTdMT constructs to gain insight into the structural and functional properties of the native protein.

Specific aims are:

- Introduction of mutations into the cys-x-cys motifs in the alpha- and beta-domains of GSTdMT in accordance with a pattern observed in the alpha domain of vertebrate MTs.
- Verification of expression of the mutant proteins in E. coli.
- Purification of the mutant proteins.
- Biophysical characterization of the mutants by native- and SDS-PAGE, ICP-OES, tryptic digestion, dynamic light scattering and SAXS.
- Determination of the effect of mutations on the Cd-binding properties and structural features of the durum MT.

2. OVERVIEW

2.1. Metallothionein (MT) Proteins

2.1.1. General Information

MTs is a name for a superfamily of low molecular weight (6-7 kDa) cys-rich proteins containing sulfur-based metal clusters. It was discovered in 1957, when Margoshes and Vallee identified a cadmium-binding protein responsible for the natural accumulation of cadmium in equine kidney cortex (Margoshes & Vallee, 1957; Pulido *et al*., 1960). Although MTs are widely distributed among the animal and plant kingdoms, they are found in eukaryotic and prokaryotic microorganisms as well (Kagi *et al*., 1991; Vasak & Hassler, 2000; Vasak & Romero-Isart, 2002; Vasak & Romero-Isart, 2005).

They preferentially contain d^{10} metal ions, as a result of polarizable cysteine thiolate ligands. Clusters are usually formed by their coordination to arrays of closely packed cys-thiolate groups (Kagi & Shaffer, 1988). Although naturally occurring MTs are most commonly isolated with Zn(II), Cd(II) and Cu(II), a number of metal ions bind to the protein in vitro. These include Ag(I), Au(I), Bi(III), Co(II), Fe(II), Hg(II), Ni(II), Pt(II), and Tc(IV)O. The affinity of the metal ions for the binding sites follows the order found for inorganic thiolates, i. E. Hg(II)>Ag(I), Cu(I)>Cd(II)>Zn(II) (9) (Vasak & Romero-Isart, 2002).

2.1.1.1. Nomenclature of MT

The first nomenclature of MTs was generated at The First International Meeting on Metallothionein and Other Low Molecular Weight Metal-Binding Proteins in 1978. Moreover, at the Second International Meeting on Metallothionein and Other Low Molecular

Weight Metal-Binding Proteins, in 1985, the adapted version was presented by the Committee (Kojima *et al*., 1997).

Based on the characteristics of the first protein that was isolated from horse kidney, committee made a definiton for MTs in 1985: "Polypeptides resembling equine renal metallothionein in several of their features can be designated as metallothionein." All polypeptides fitting this definion are termed as metallothionein.

2.1.1.2. Classes and Types of MT

Metallothionein superfamily was divided into three classes by the committee established in 1985. Class I MTs contain 20 highly conserved Cys residues based on mammalian MTs and are widespread in vertebrates. MTs without this strict arrangement of cysteines are referred to as Class II MTs and include all those from plants and fungi as well as nonvertebrate animals. In addition, Class III MTs contain all other similar polypeptides that are enzymatically synthesized (Klaasen, 1999; Cobbett & Goldsbrough, 2002).

MTs are currently clustered in 15 families based on phylogenetic relationships (Kojima, Binz & Kagi, 1999).

Family 1: vertebrate MTs
m1: mammalian MT-1
m2: mammalian MT-2
m3: mammalian MT-3
m4: mammalian MT-4
m: n.d. mammalian MT
a1: avian MT-1
a2: avian MT-2
a: n.d. avian MT
b: batracian MT
t: teleost MT

Family 2: mollusc MTs
mo1: mussel MT-1
mo2: mussel MT-2
mog: gastropod MT
mo: n.d. mollusc MT

Family 3: crustacean MTs
c1: crustacean MT-1
c2: crustacean MT-2
c: n.d. crustacean MT

Family 4: echinodermata MTs
e1: echinodermata MT type 1
e2: echinodermata MT type 2

Family 5: diptera MTs
d1: diptera MT type 1
d2: diptera MT type 2

Family 6: nematoda MTs
n1: nematoda MT type 1
n2: nematoda MT type 2

Family 7: ciliata MTs
ci: ciliata MT

Family 8: fungi-I MTs
f1: fungi-I MT

Family 9: fungi-II MTs
f2: fungi-II MT

Family 10: fungi-III MTs
f3: fungi-III MT

Family 11: fungi-IV MTs
f4: fungi-IV MT

Family 12: fungi-V MTs
f5: fungi-V MT

Family 13: fungi-VI MTs
f6: fungi-VI MT

Family 14: prokaryota MTs
pr: prokaryota MT

Family 15: planta MTs
p1: plant MT type 1
p2: plant MT type 2
p2v: plant MT type 2 variant, described as a clan of p2
p3: plant MT type 3
p21: plant MT type 2x1
pec: plant EC MT-like protein

Family 99: phytochelatins and other non-proteinaceous MTs

Figure 2.1: Defined MT families and subfamilies (Binz & Kagi, 1999).

2.1.1.2.1. Cysteine Residue Distribution or Source Organism

The characteristic feature of all MTs is the abundance of cys and their arrangement in chelating cys-cys, cys-x-cys, cys-x-y-cys, and cys-cys-x-cys-cys where x and y stands for an amino acid residue other than Cys (Kagi & Shaffer, 1988; Vasak & Romero-Isart, 2002).

The conservation of these clusters in an increasing number of three-dimensional structures of invertebrate, vertebrate and bacterial MTs signifies the importance of this structural motif (Vasak, 2005).

2.1.1.2.2. Mammalian MTs

The mammalian MTs are characterized by a molecular weight of 6000-7000. They are composed of around 60 amino acids and binding a total of 7 equiv of bivalent metal ions. Aromatic amino acid residues are absent as well. All 20 cys, among 60 amino acids, are deprotonated and participate in metal binding through mercaptide bonds (Kagi & Shaffer, 1988).

In mammalian cells, the protein is most abundant in parenchymatous tissues, namely liver, kidney, pancreas, and intestines (Kagi & Shaffer, 1988). The binding of copper to MT plays mainly a role in copper sequestration in copper-related disorders such as the Menkes and Wilson disease. In addition to their role in metal-related cellular processes, they involve in a number of biological processes, like protection against reactive oxygen species, adaptation to stress, protection against brain injury, antiapoptotic effects or regulation of neuronal outgrowth (Andrews *et al*., 2000; Vasak & Hasler, 2000; Moffatt & Denizau, 1997; Hidalgo *et al*., 2001).

In recent years, there is an increasing interest in the function of these proteins in the brain. MT-1/MT-2 expression is sharply increased in response to central nervous system (CNS) injury and also in neurodegenerative diseases such as Alzheimer's disease (AD). It has been established that MT-1/MT-2 are able to directly reduce the inflammatory response associated with CNS injury, leading to enhanced recovery (Vasak, 2005).

2.1.1.2.3. Non-mammalian MTs

In recent years, the variety of known MTs has expanded dramatically. An increasing number of new amino acid sequences of MTs from various species is being reported.

"Probably the most interesting new MT forms were found in the snail *Helix pomatia*" Dallinger wrote in 1997. Terrestrial snails can tolerate very high concentrations of cadmium in the midgut gland and accumulate relatively high amounts of copper in the foot and mantel. Surprisingly, the specific metal accumulation in these tissues is the consequence of tissue-specific MT isoforms. Both of them contains 18 conserved cys-residues but there is a difference between other amino acids (Dallinger *et al*., 1997).

2.2. Structural Characteristics of MT Proteins

It is the cys-residues that form thiol bonds with metal ions to stabilize the structure. The metal-free protein, thionein, appears to possess a disordered structure (Romero-Isart & Vasak, 2002). However a basic fold for the apoprotein is predicted by molecular modeling calculations (Rigby & Stillman, 2004).

Moreover, the mobility of the protein backbone structure enfolding the metal core in mammalian MTs is well-documented (Vasak *et al*., 1994; Kagi, Riordan, & Vallee, 1991). Both the calculated RMSD values from NMR data and the crystallographic B-factors indicate that a considerable degree of dynamic structural disorder exists (Robbins *et. al*., 1991; Schultze *et. al*., 1988). Recent model calculations indicate also the involvement of residues other than cys in establishment of the protein fold (Romero-Isart et al., 2010).

The crystal structure of rat $C_{5,}Zn_2$-MT-2 and the solution NMR structures of $^{113}Cd_7$-MT-2 from rabbit are the first elucidated three-dimensional MT structures (Figure 2.2). They showed identical metal-thiolate cluster structures and a monomeric dumbbell shaped protein with seven metal ions located in two separate clusters. A hinge region is composed of a conserved Lys-Lys segment (Vasak, 2005). In contrast, for the yeast MT, residues of both regions form a single joint cluster (Furey *et. al*., 1986; Sayers *et. al*., 1999).

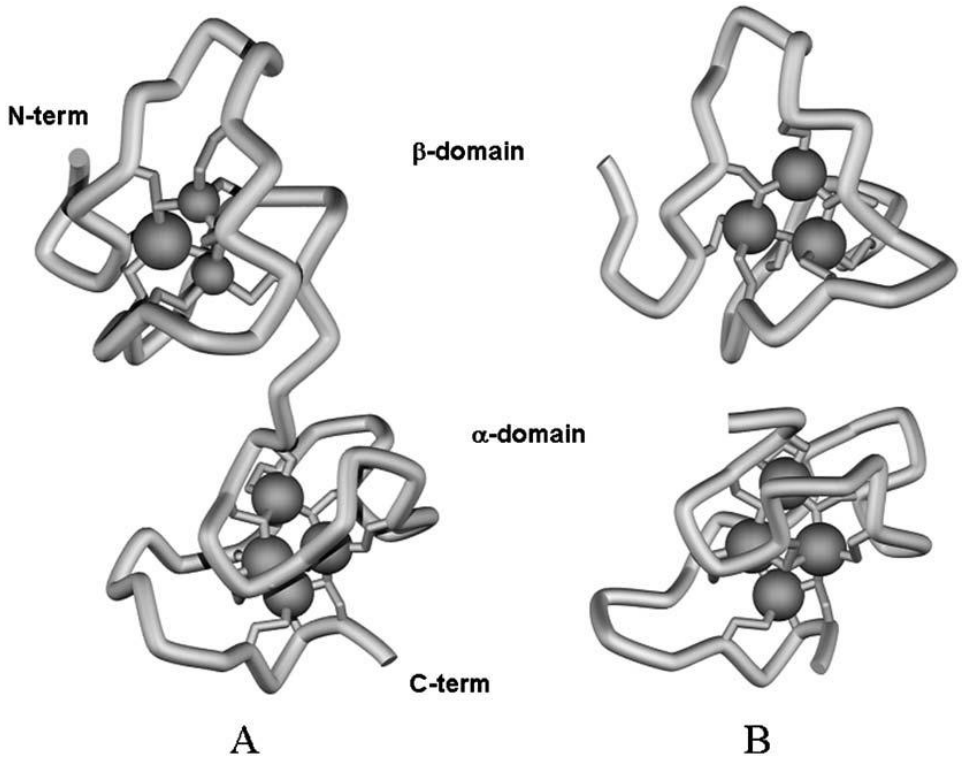

Figure 2.2: Three-dimensional structure of rat MT2 as determined by (A) X-Ray crystallography, C_5Zn_2-MT-2, and (B) by NMR in aqueous solution $^{113}Cd_7$-MT-2. Metals are shown as shaded spheres connected to the protein backbone by cys-thiolate ligands (Vasak, 2005).

Models for the spatial structure of mammalian MT and the organization of the metal-thiolate clusters have recently been derived from 2D NMR spectroscopic measurements in aqueous solution (Braun *et al*., 1986; Arseniev *et al*., 1988; Schultze *et al*., 1988) and from X-ray diffraction data obtained on crystals (Furey *et al*., 1986).

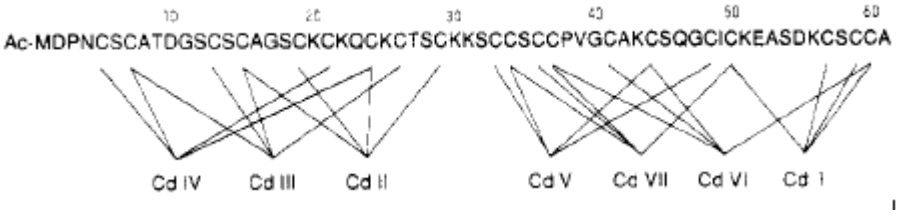

Figure 2.3: Cadmium-cysteine connectivities of rat liver metallothionein 2 as established by two-dimensional 1H113Cd NMR spectroscopy (adapted from Vasak *et al*., (1987)).

The stabilization by a total of 42 cys-metal-cys cross links is the special characteristic of the mammalian MTs. 24 of these connections in the alpha-domain and 18 in the beta-domain, the conformational stability and the collective affinity for the metal are expectedly lower in the latter. Hence, the cys side chains of the beta-domain are more accessible to alkylating agents and has a greater tendency to lose metal (Bernhard *et al*., 1986).

2.3. Plant MTs

2.3.1. Classification of Plant MTs

The first cys-rich small protein was isolated from plant material and named as MT almost 25 years ago (Hanley-Bowdoin & Lane, 1983). Until now, the number of plant MT sequences has increased enormaously and 25 % of all metallothionein entries in the Swiss-Prot protein sequence database are plant metallothioneins.

Plant MTs differ from animal MTs with respect to the two short cys-rich terminal domains, a long cys-devoid spacer regions between them, and the presence of aromatic amino acids. In contrast, most other MTs have a spacer region of less than 10 amino acids that do not include aromatic residues. Plant MTs are placed in Family 15 of the MT superfamily. They are further categorized into four types according to the cystein residue distribution by Cobbet and Goldsbrough (Rauser, 1999; Cobbett & Goldsbrough, 2002). This classification is able to place almost all of the known plant MT genes into four categories based on amino acid sequence (Figure 2.4).

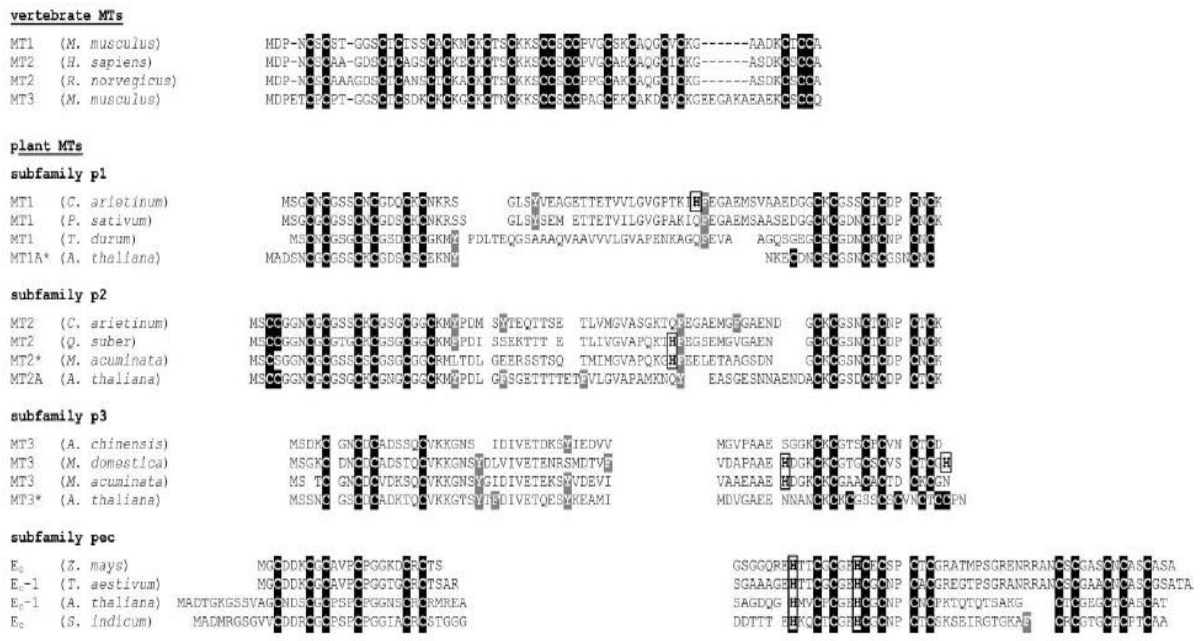

Figure 2.4: Amino acid sequence alignment of representative members of the vertebrate MT family as well as of the four subfamilies. Cys residues are highlighted with a black background , aromatic amino acids with a grey background. His residues are framed with a black border. Sequences denoted with * represent exceptions to the otherwise highly conserved Cys distribution pattern within a plant MT subfamily . In A. thaliana MT1A the linker region is additionally reduced to just seven amino acids (Freisinger, 2008).

The first three subfamilies have less cys residues and these residues are clustered in two cys-rich domains with longer linker regions, whereas the fourth subfamily have three cysteine-rich domains.

MT1 contains six Cys-X-Cys motifs in total and are distributed equally among two cys-rich domains. The two domains are separated by approximately 40 amino acids that contains Phe and Tyr residues and also His.

Similar to MT1, MT2 has two cys-rich domains that are separated by 40 amino acid linker region. However, the first pair of cys-motif is present as a Cys-Cys motif in amino acid positions 3 and 4 of these proteins. A Cys-Gly-Gly-Cys motif is present at the end of the N-terminal cys-rich domain as well. Moreover, MSCCGGNCGCS sequence of the N-terminal domain of MT2 is highly conserved. Despite of the difference of cys-motifs in the N-

terminal, the C-terminal domain contains three Cys-X-Cys motifs. In addition, the linker region of MT2 is much more variable between species.

MT3 contains less cys residues in the N-terminal domain, only four exist. The consensus sequence for the first three is Cys-Gly-Asn-Cys-Asp-Cys. The fourth cysteine is not part of a pair of cys but is contained within a highly conserved motif, Gln-Cys-X-Lys-Lys-Gly. However, three Cys-X-Cys motifs are seen in the C-terminal. Same as MT1 and MT2, the linker region of MT3 is approximately 40 amino acid long.

MT4 (pec) differs from other plant MTs by having three cys-rich domains, each containing 5 or 6 conserved cys residues, which are separated by 10 to 15 amino acid long linker regions. Most of the cys are present as Cys-X-Cys motifs. Although a large number of MT4 members have not been identified, compared to those from monocots, MT4 from dicots contains an additional 8 to 10 amino acids in the N-terminal domain before the first cysteine residues (Cobbett & Goldsbrough, 2002).

2.3.2. Function of Plant MTs

The expression of plant MT genes has been characterized in many kinds of tissues. However, they have some general trends. MT-1 expressed predominantly in roots, MT-2 in leaves, MT-3 in fruits and MT-4 in seeds (Zhou & Goldsbrough, 1994; Hsieh *et al*., 1995; Zhou & Goldsbrough, 1995; Hsieh *et al*., 1996; Guo *et al*., 2003).

More than 5 decades after the discovery of the first plant MT, little is known regarding the possible functions and properties of plant MTs.

Once inside plant cells, metals in excess need to be stored to prevent their toxicity. This is invariably linked to the existence of specific metal-binding macromolecules (Kagi & Shaffer, 1988) and metallothioneins (MTs) are proteins that responsible for metal ion-storage and detoxification (Briat & Lebrun, 1998).

As a result of their unusual metal binding properties, the functions of plant MTs presumably include the involvement in homeostasis of essential trace metals, zinc and copper or sequestration of the environmental toxic metals cadmium and mercury (Vasak & Romero-Isart, 2002; Vasak *et al*., 2005). In addition, accumulation of metallothionein in response to

elevated metal ion concentrations, and its association with these ions may indicate a role in the sequestration of excess metal (Robinson *et al*., 1993).

Synthesis of metallothionein increases following exposure to elevated concentrations of Cu^{+} and Ag^{+} in fungal cells (Karin *et al*., 1984; Fürst *et al*., 1988), Cd^{2+} and Zn^{2+} in cyanobacteria (Olafson *et al*., 1988), and a range of trace metals including the ionic species of cadmium, zinc, copper, mercury, gold, silver, cobalt, nickel, and bismuth in animals (Robinson *et al*., 1993). An increasing body of evidence suggests that plant MTs fulfil different functions.

2.3.3. Structure and Metal Binding Properties of Plant MTs

In contrast to the huge amount of knowledge about the structure of animal MTs from a number of NMR solution studies as well as single crystal X-Ray diffraction, the structural and functional properties of plant MTs are still largely unknown (Robinson *et al*., 1993; Cobbett & Goldsbrough, 2002).

There are several significant reason of this case. Crystallization of MTs is a challenging task due to the high number of cys-residues in a relatively small molecular weight and oxidation sensitivity of protein. Moreover, MTs lack secondary structural elements, they have a highly dynamic structure. In addition to all, plant MTs have longer hinge region that is sensitive to proteolytic claevage and this impedes the recombinant protein expression.

Question of whether members of the plant MT1, MT2, and MT3 subfamilies form a single cluster or two separate clusters is still not known.

A novel Type I plant MT gene (*dmt*) in *Triticum durum* was identified and cloned for overexpression in *E.coli* (Bilecen *et al*., 2005). *T. durum* metallothionein (dMT) displays three sequence domains: metal binding N terminus (β domain, 1-19th residues) and C terminus (α domain, 61-75th residues) and a long hinge region (20-60th residues). Cysteines are clustered equally in N and C termini with a Cys-X-Cys motif (Cys-motif) and the hinge region possess no Cys residues. dMT was overexpressed in *E.coli* as a GST (glutathione-S-transferase) fusion protein (GSTdMT). Both GSTdMT and dMT cleaved from GST were purified and characterized by biochemical and biophysical methods. It was shown that GSTdMT binds

3.5±1 moles of Cd per one mole of protein and has a high tendency to form stable oligomeric structures (Yesilirmak, 2008). The structure of GSTdMT and dMT were investigated by small angle X-ray scattering (SAXS) and computational methods. According to SAXS results, GSTdMT existed as a dimer and dMT has an elongated structure. Homology modeling indicated that dMT has two separate clusters which correlates with the SAXS results. Moreover, the existence two separate clusters was proposed for *Tricium aestivum* Ec-1 metallothionein as well according to the limited proteiolytic digestion, mass spectrometry, and amino acid analysis (Peroza & Freisinger, 2007).

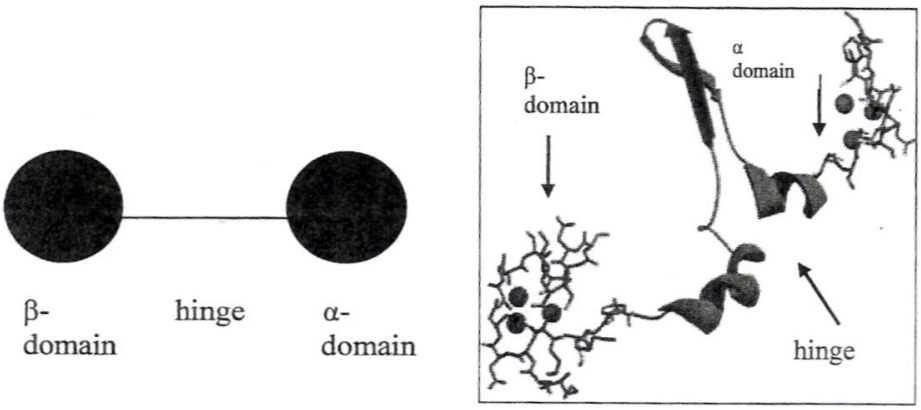

Figure 2.5: (A) Schematic representation of the dumbbell model (Collak, 2009). (B) Predicted structure of dMT (Bilecen *et al*., 2005). Metal centers are presented in ball and stick presentation and the hinge region is depicted in ribbon presentation.

On the other hand, a hairpin model was proposed for a Type II MT *Quercus suber* MT (QsMT). It has a 38 amino acids long hinge region and two cys-rich beta and alpha domains. According to data obtained from ESI-MS, ICP-OES, CD, UV-vis spectropolarimetry of recombinant Zn and Cu bound beta and alpha domains and a chimera in which hinge is replaced by four glycine of QsMT, beta and alpha domains form a single cluster and the hinge region does not contribute to the metal binding (Domenech e*t al*., 2007). The hairpin model was proposed for a pea MT $PsMT_A$ as well (Kille, Winge, Harwood, & Kay, 1991).

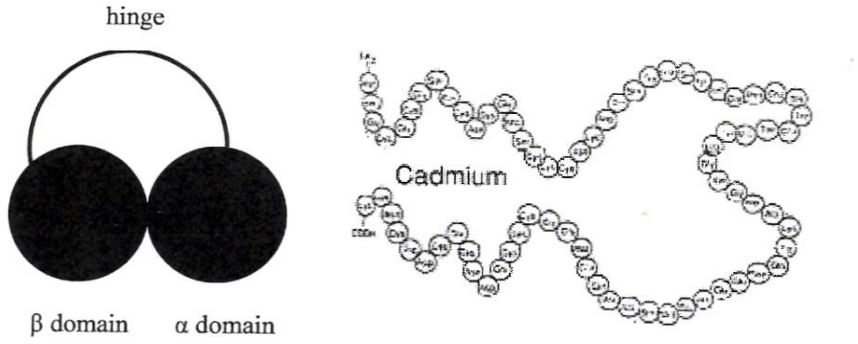

Figure 2.6: (A) Schematic representation of hairpin structure of MTs (B) Proposed hairpin structure of pea MT, $PsMT_A$ (Adapted from Kille *et al*., 1991).

3. MATERIALS AND METHODS

3.1. Materials

3.1.1. Chemicals

All chemicals were supplied by Stratagene, Qiagen, Merck (Germany), Bioron, Fermentas, Riedel, Amresco, AppliChem, and SIGMA (USA).

3.1.2. Primers

Primers were designed according to the sequence of dMT (Bilecen *et al*., 2005) and synthesized by Iontek (Turkey). Primer sequences are shown in Table 3.1.

Sequence	Mutation
5’- AAC TGT GGA TCC TGT TGC AGC TGC TGC TCA GAC TGC AAG -3’	**G61CG65C**
5’- CTT GCA GTC TGA GCA GCA GCT GCA ACA GGA TCC ACA GTT -3’	
5’- CAG TCC GGC GAG TGC TGC AGC TGC TGC GAC AAC TGC AAG -3’	**G8CG12C**
5’- CTT GCA GTT GTC GCA GCA GCT GCA GCA CTC GCC GGA CTG -3’	
5’- AAC TGT GGA TCC TGT TGC AGC TGC GGC-3’	**G8C**
5'- GCC GCT GCA ACA GGA TCC ACA GTT -3'	
5’-AGC TGC TGC TCA GAC TGC AAG TGC GGG-3’	**G12C**
5’- CCC GCA CTT GCA GTC TGA GCA GCA GCT -3’	
5’- CAG TCC GGC GAG TGC TGC AGC TGC GGC -3’	**G61C**
5’- GCC GCA GCT GCA GCA CTC GCC GGA CTG -3’	
5’- GGC TGC AGC TGC TGC GAC AAC TGC AAG -3’	**G65C**
5’- CTT GCA GTT GTC GCA GCA GCT GCA GCC -3’	

Table 3.1: Primers used in the Site-Directed Mutagenesis of GSTdMT.

3.1.3. Enzymes

Restriction enzymes *Eco*RI, *Xho*I, and *Dpn*I were purchased from Strategene and Fermentas. Moreover, Pfu-Turbo DNA polymerase was supplied by Stratagene.

3.1.4. Vectors

Map of pGEX-4T2 (GE Healthcare) vector can be found in Appendix B.

3.1.5. Cells

E. coli strains XL1 Blue (Stratagene), BL21(DE3), Rosetta(DE3), and Rosetta(DE3)pLysS (provided by EMBL, Hamburg) were used.

3.1.6. Buffers and Solutions

All buffers and solutions, except those provided by commercial kits were prepared according to Sambrook et al., 1989. Buffers and their compositions are given in Appendix C.

3.1.7. Commercial Kits

Quick Change Site-Directed Mutagenesis Kit (Stratagene) and Qiaprep Spin Miniprep Kit (QIAGEN) were used in recombinant DNA manipulations.

3.1.8. Culture Media

3.1.8.1. Liquid and Solid Medium

LB (Luria-Bertani) Broth from SIGMA was used to prepare liquid culture media for bacterial growth. The components of LB Broth are 10 g Tryptone, 5 g Yeast extract, and 5 g NaCl for 1 liter.

LB (Luria-Bertani) Broth Agar form SIGMA was used for the preparation of solid culture media for bacterial growth. The components of LB Broth are 10 g Tryptone, 5 g Yeast extract, 5 g NaCl, and 15 g Agar for 1 liter.

3.1.9. Equipments

Please see Appendix D for a complete list of all equipments that were used during this study.

3.2. Methods

3.2.1. Site-Directed Mutagenesis

3.2.1.1. PCR

Recommended reaction volumes and final concentrations of the Quick Change Site-Directed Mutagenesis Kit were used for PCR reaction mixture.

Reaction was carried out in a Thermocycler following below conditions (Table 3.2 and 3.3).

95 ^{o}C, 1 minute	
95 ^{o}C, 30 second	A total of 20 cycles
55 ^{o}C, 1 minute	
68 ^{o}C, 10 minute	
4 ^{o}C, hold forever	

Table 3.2: PCR conditions used for double mutation of GSTdMT.

95 ^{o}C, 1 minute	
95 ^{o}C, 30 second	A total of 20 cycles
55 ^{o}C, 1 minute	
68 ^{o}C, 10 minute	
68 ^{o}C, 4 minute	
4 ^{o}C, hold forever	

Table 3.3: PCR conditions used for single mutations of GSTdMT.

PCR products were analysed by 1% agarose gel electrophoresis with TAE buffer. Samples were mixed with 6X loading buffer and gels were run at 100 mV constant voltage for 30 minutes. Size of DNA fragments were estimated by using MassRuler DNA ladder mix (Fermentas) and visualized by ethidium bromide staining.

3.2.1.2. *Dpn*I Digestion

*Dpn*I restriction enzyme cleaves only methylated DNA. The template is derived from an alkaline lysis plasmid preparation and it is methylated, whereas the mutated PCR product is generated in vitro and is unmethylated. Hence, enzyme will only cleaves unmutated plasmid and leaves mutated ones as they are.

1.5 μl of *Dpn*I restriction enzyme (10U/μl) was added directly to each amplification reaction. They were incubated immediately at 37 ^{o}C for 2 hour.

3.2.1.3. EtOH Precipitation

PCR products were concentrated by ethanol precipitation. 1 volume of ddH_2O was added to each reaction to increase the initial volume. 0.1 volume of 3M ammonium acetate was then added in order to increase the positive ion concentration. Then, 2 volume of 95 % EtOH was immediately added and they were incubated at -80 ^{o}C for o/n. Next day, the solution was centrifuged for 15 min at full speed to eliminate salts. Pellet was washed with 2 volume of 70 % EtOH and was centrifuged for 15 min at full speed again. Lastly, they were allowed to dry and resuspended with 5 μl of ddH_2O very carefully.

3.2.1.4. Transformation

EtOH precipitated linear PCR products were transformed in BL21(DE3) competent cells. 80 μl of *Dpn*I treated PCR products were gently added to the 100 μl of competent cells and the tube was incubated on ice for 30 minutes, then they were allowed to repair on pre heated 42^{o}C rack for exactly 90 seconds, then again on ice for 2 minutes. Finally, they were allowed to reproduce in LB at 37^{o}C for 45 – 60 minutes. Then, transformed cells and controls were plated on LB-Ampicillin (100 mg/ml) plates.

3.2.1.5. Colony Selection

Positive colonies were selected and grown on liquid LB-Ampicillin (100 μg/ml) for both preparing glycerol stocks and plasmid isolation.

3.2.1.6. Plasmid Isolation

Positive colonies were grown in 5 ml of LB-Ampicillin (100μg/ml) medium overnight at 37 ^{o}C with shaking at 280 rpm. Cells were centrifuged at 4^{o}C at 5000 g for 3 minutes and plasmid isolation was done with Qiaprep Spin Miniprep Kit (QIAGEN). The final concentration of plasmid DNA was calculated by measuring the absorbance at 260 nm in Nanodrop spectrophotometer. DNA samples were stored at -20 ^{o}C.

3.2.1.7. Restriction and Agarose Gel Electrophoretic Analysis

Purified plasmids were checked by restriction and agarose gel electrophoretic analysis for the presence of mutant inserts. Plasmids were digested with *Eco*RI and *Xho*I restriction enzymes to verify the presence of GSTdMT gene. 0.3 μl of *Eco*RI and 0.6 μl of XhoI restriction enzymes were added to approximately 10 ng template. They were incubated immediately at 37 ^{o}C for 2 hours.

3.2.1.8. Sequence Verification

The plasmids were purified with QIAGEN Plasmid Mini Kit (QIAGEN) and were DNA sequence analysis was carried out by Iontek (Turkey).

3.2.2. Protein Expression

3.2.2.1. Monitoring the Expression of the Mutant Proteins

In order to monitor the expression of the mutant proteins, cells were grown in 5 ml of LB-Ampicillin (100 μg/ml) medium overnight at 37 ^{o}C with shaking at 280 rpm. Next day, cultures were 1:50 diluted in 50 ml of LB-Ampicillin (100 μg/ml) medium and induction was obtained with 0.7 mM IPTG when the OD_{600} was around 1. Cells were grown continuously at 37 ^{o}C with shaking at 280 rpm. Induction was monitored by taking aliquots from the cultures before induction (t=0) and after induction at regular intervals for a maximum of about 7 hours (t=1, 2…) and pelleting the cells. Pellets were lysed in the lysis buffer (150 mM NaCl, 20 mM Hepes, 2.5 mM $MgCl_2$, 10mg/ml lysozyme, pH8) and

expression was monitored by 12% SDS polyacrylamide gels. Gels were first run at 80 V and after the bands entered the separating gel the voltage was increased to 120 V for around 1 hour 30 minutes. Protein bands were visualized by coomassie blue stainig. Protein molecular weight markers and protein ladders (Fermentas) were used to identify the molecular weights of expressed proteins.

3.2.2.2. Culture Growth for Purification

Large scale purification of mutant proteins was carried out from 2.25 liter cultures. Each one was grown in 50 ml of LB-Ampicillin (100 μg/ml) medium overnight at 37 ^{o}C with shaking at 280 rpm. Next day, cultures were 1:50 diluted in 2.25 liter of LB-Ampicillin (100 μg/ml) medium containing 0.1 mM $CdCl_2$. Induction was obtained with 0.7 mM IPTG when the OD_{600} was around 1. Cells were grown continuously at 37C with shaking at 280 rpm for 5.5 hours and pelleted by centrifugation at 7000 rpm for 30 minutes using a Sorvall centrifuge with SLA 3000 rotor or at 7000 rpm for 20 minutes using a Sorvall untracentrifuge. Pellets were kept at -80 ^{o}C until further use.

3.2.3. Purification

3.2.3.1. Affinity Chromatography

Purification experiments were performed under argon-saturated conditions. Pellets were resuspended in 20 mM Hepes, pH 8.0, 2.5 mM $MgCl_2$, 100 mM NaCl, 1 mM DTT, 0.5 mM PMSF, 0.1 mM $CdCl_2$, and 2 tablet of EDTA-free protease inhibitor. All cells were lysed by 10 minutes of sonication at 4 ^{o}C with 5 second of pulse and 5 second of waiting period. 20 % Triton X-100 was added, a final concentration of 1%, and the mixture was shaken gently at 4^{o}C for 45 minutes. Lysate was centrifuged at 13000 rpm, 4 ^{o}C for 1 hour. The 5 ml GSTrap FF affinity column (GE Healtcare) was previously washed with 25 ml Hepes buffer with 1 mM DTT. The column was then connected to an AKTA-FPLC system (GE Healthcare) during the elution step. About 80 ml of supernatant was loaded the column and 50 mM Tris-HCl, pH 8.0 with 20 mM reduced glutathione was used for elution of GSTdMT at 1 ml/min collecting 1-ml fractions. Then, the fractions were pooled and dialysed

against Hepes buffer with 1 mM DTT and 0.5 mM PMSF overnight with three changes of buffer.

3.2.3.2. Size Exclusion Chromatography

Dialysed protein was loaded on a Hiload 16/60 Superdex 75 (GE Healthcare). The size exclusion column was calibrated using Vitamin B12, Ribonuclease A, Chymotrypsinogen A, Ovalbumin, and BSA. The calibration curve (not shown) was used for molecular weight determination of mutant proteins. Column eluate was collected at a speed of 1 ml/min in 0.5 ml fractions and monitored by A280 measurements using the AKTA-FPLC system (GE Healthcare).

3.2.4. Analyses

3.2.4.1. Protein Concentration Determination

Protein concentration was determined using the relationship A280=0.5 for A280 values and UVvis absorbance spectra were measured using a nanodrop.

3.2.4.2. SDS and Native Polyacrylamide Gel Electrophoresis (PAGE)

SDS gels were prepared according to the recepies given in Appendix C (Laemmli, 1974). In order to equalize the amount of proteins on the gel, 5μl sample was taken from the top fraction of the size exclusion chromatography and volume of the other samples were decided based on the concentrations of each fraction. Protein samples were mixed with 2X SDS-PAGE sample buffer (0.125 mM Tris-HCl pH 6.8, 4 % SDS, 20 % glycerol, 10 % betamercaptoethanol, 0.04 % bromophenol blue), heated at 95 ^{o}C for 3 minutes, and loaded into 12 % SDS polyacrylamide gels having 5 % of stacking gel. Gels were run at 80 V in 1X SDS running buffer (25 mM Tris, 192 mM glycine, 0.1 % (w/v) SDS). When the bands entered the separating gel the voltage was increased to 120 V for approximately 1 hour 30 minutes.

Native gels were prepared according to the recepies given in Appendix C. Similar to SDS-PAGE, to load the same amount of proteins on the gel, 5μl sample was taken from the top fraction of the size exclusion chromatography and volume of the other samples were decided according to the concentrations of each fraction. Protein samples were mixed with 2X Native-PAGE sample buffer (0.125 mM Tris-HCl pH 6.8, 20 % glycerol, 10 % betamercaptoethanol, 0.04 % bromophenol blue) and loaded into 10 % Native polyacrylamide gels without heating. Gels were run at 80 V in 1X Native running buffer (25 mM Tris, 192 mM glycine) until the samples passed from stacking gel. Then, the voltage was increased to 120 V for almost 1 hour 30 minutes.

3.2.4.3. Tris-Tricine Polyacrylamide Gel Electrophoresis (PAGE)

Gels were prepared according to the recepies given in Appendix C. 10μl protein samples were mixed with 2X SDS-PAGE sample buffer (0.125 mM Tris-HCl pH 6.8, 4 % SDS, 20 % glycerol, 10 % betamercaptoethanol, 0.04 % bromophenol blue), heated at 95 ^{o}C for 3 minutes, and loaded into 16 % Tris tricine gels having 5 % of stacking gel. Gels were run at 80 V in 1X SDS running buffer (25 mM Tris, 192 mM glycine, 0.1 % (w/v) SDS). When the bands entered the separating gel the voltage was increased to 120 V for approximately 2 hour 30 minutes.

3.2.4.4. Coomassie Blue and Silver Staining

For visualization, SDS- and Native- polyacrylamide gels were stained with coomassie blue solution and destained in distilled water. The recepie of coomassie blue solution is given in Appendix C.

For silver staining, recommended reaction volumes and procedures given in the instructions for the Biorad Silver Staining Kit were used for visualization of Tris tricine gels with silver.

3.2.4.5. Thrombin Cleavage

3.2.4.6.1. Small Scale Cleavage

Approximately 0.3 mg of purified protein was incubated with 3U of thrombin in the cold room. After overnight incubation, the cleaved proteins were analysed by 16 % Tris tricine gels.

3.2.4.6.2. Large Scale Cleavage and Purification of the Cleaved Protein

Pellets were resuspended in 20 mM Hepes, pH 8.0, 2.5 mM $MgCl_2$, 100 mM NaCl, 1 mM DTT, 0.5 mM PMSF, 0.1 mM $CdCl_2$, and 2 tablets of EDTA-free protease inhibitor. All cells were lysed by 10 minutes of sonication at 4 ^oC with 5 second of pulse and 5 second of waiting period. Total sonication period was 20 minutes. 20 % Triton X-100 was added, a final concentration of 1 %, and the mixture was shaken gently at 4 ^oC for 45 minutes. Lysate was centrifuged at 13000 rpm, 4 ^oC for 1 hour. The supernatant was incubated with glutathione sepharose 4B beads for 4 hours at 4 ^oC with gentle shaking. Then, the beads were centrifuged and washed with Hepes buffer three times to discard the unbound proteins and 375 U thrombin was added to the beads for incubation of 16 hours at 4 ^oC on a rotating plate.

After 16 hours, the beads were centrifuged and the supernatant was concentrated using centriprep YM-10 (Amicon) with 10.000 MWCO at 3000 g, 4 ^oC until 2 ml of sample was obtained. Concentrated protein was loaded on a Hiload 16/60 Superdex 75 (GE Healthcare). Column eluate was collected at a speed of 1 ml/min in 0.5 ml fractions and monitored by A280 measurements using the AKTA-FPLC system (GE Healthcare).

3.2.4.6. Limited Proteolytic Cleavage with Trypsin

Trypsin is a serine protease which cleaves peptides at the carboxyl side of lysine or arginine when either is followed by a proline. 100 μg of purified protein was incubated at 30 ^oC for 30 minutes while shaking at 300 rpm. Then, 8 μl of 0.0025 mg/ml trypsin in trypsin buffer (20 mM Hepes, pH 8, 2.5 mM $MgCl_2$, 10 mM KCl, 2 mM DTT) was added to the protein. In order to follow the cleavage pattern, samples were collected at 30

seconds, 1-5-10-30 minutes, 1 hour, and after overnight incubation. In order to stop the reaction 10mM PMSF was added to each sample. They are stored at 4 ^{o}C and then analysed by 16 % Tris tricine gel.

3.2.4.7. Dynamic Light Scattering (DLS)

Fractions of mutant proteins were analyzed by DLS using Zeta-Sizer Nano ZS (Malvern Instruments). This system determines the size of the particles in a solution by measuring the Brownian motion of the particles by dynamic light scattering. Changes in the position of the scattered light due to Brownian motion of particles are correlated with the diffusion speed which in turn is used to calculate the size.

Small particles move more quickly while large particles move more slowly. Stokes-Einstein equation defines the relationship between the size of a particle and its speed due to Brownian motion. The velocity of Brownian motion is determined by translational diffusion coefficient. As large particles move slowly, the intensity of the speckle pattern will also fluctuate slowly. In contrast, the intensity of the speckle pattern will fluctuate quickly for small particles as they move more quickly.

First size distribution generated by DLS is an intensity distribution. It is then converted to volume and number distributions. According to the Rayleigh approximation, the intensity of scattering of a particle is proportional to the sixth power of its diameter. That's why the most reliable analysis is an intensity distribution since the difference between scattering of small and large particles are much more than their difference in number or volume distribution.

3.2.4.8. Circular Dichroism Spectropolarimetry (CD)

Circular dichroism (CD) spectropolarimetry measures the difference between the absorption of left handed and light handed polarized light that occur because of the asymmetry of the structure. While ordered structures can give both positive and negative signals, the absence of regular structure results in zero intensity.

CD spectropolarimetry can be used to determine whether a protein is folded and its secondary and tertiary structural elements can be characterized. In the far-UV spectral

region (190-250 nm) secondary structures can be determined whereas in the near-UV spectral region (250-350 nm) clues regarding the tertiary structure could be gained. At far-UV wavelengths, the signal arises when the peptide bond is folded. Alpha-helix, beta-sheet, and random coil structures give rise to a characteristic shape and magnitude of CD spectrum. Overall, the CD signal reports an average of the protein, in other words, CD can determine that a protein contains about 50% alpha-helix, but it cannot determine which specific residues are involved in the alpha-helical portion. At near-UV region, the aromatic amino acids and disulfide bonds create signals. Signals from 250-270 nm are attributable to phenylalanine residues, signals from 270-290 nm are attributable to tyrosine, and 280-300 nm are attributable to tryptophan. Disulfide bonds give rise to broad weak signals throughout the near-UV spectrum.

3.2.4.9. Inductively Coupled Plasma Optical Emission Spectroscopy (ICP-OES)

ICP-OES is a major analytical method for element analysis. The sample is dissociated into its atoms and ions by a high temperature radio frequency induced argon plasma. Atoms and ions are excited and they emit electromagnetic radiation at characteristic wavelengths. The intensity of this emission correlates with the concentration of the element in the sample.

Concentration of the mutant proteins were calculated from A_{280} absorbance and bound Cd^{2+} was measured by Inductively Coupled Plasma Optical Emission Spectroscopy (ICP-OES, Varian, Australia) to determine the binding ratio of Cd^{2+}.

3.2.4.10. Small angle X-ray scattering (SAXS) and *ab initio* shape model determinations

Small angle X-ray scattering measurements were carried out on the EMBL X-33 beamline (Koch and Bordas, 1983) at the DORIS storage ring, DESY, Hamburg. This beamline, optimised for low background data collection from macromolecular solutions (Roessle et al., 2007), is equipped with a photon counting Pilatus 1M pixel detector (67 x 420 mm2) with a sample-detector distance of 2.7 m. During measurements samples are kept

in a vacuum cell with polycarbonate windows at 18 °C and data are collected as 3 one minute frames. Scattering patterns from different frames are compared for monitoring possible radiation damage occurring during the measurements. Data were collected from the mutant protein G61C in the concentration range 3.5 to 6.5 mg/ml in 20 mM Hepes pH 8.0, 100 mM NaCl.

The data is presented as logarithm of the scattered intensity (I(s)) against momentum transfer s ($s = 4\pi\sin\theta/\lambda$, where 2θ is the scattering angle and λ is the wavelength: 0.15 nm). Preliminary data analysis involving correction for beam intensity, background correction, buffer subtraction and concentration normalization were carried out using the PRIMUS (Konarev et al., 2003) software in the ATSAS suit of programs (Petoukhov et al., 2007) at EMBL Hamburg. Following the initial data reduction further analyses are carried out to determine the forward scattering I(0) and the radius of gyration Rg of the protein. Additionally Porod plot is calculated to obtain information about the structural flexibility of the macromolecule (Porod, 1982).

Calculations of Rg and molecular mass of the protein in solution can be carried out according to the Guinier approximation (Guinier and Fournet, 1955). Guinier approximation states that for a monodisperse solution the scattered intensity at small angles I(s) is a linear function of s^2 and the scattered intensity extrapolated to s= 0, I(0), is proportional to the molecular mass of the protein in solution. The slope of the linear fit yields the radius of gyration and for globular particles at s values where sRg <1.3;

$$\ln (I) = \ln(I(0))-s^2Rg^2 /3$$

For molecular mass (MM) determinations the scattering from a reference protein (e.g. BSA) can be used and the unknown molecular mass calculated as:

$$MM_{sample} = (I(0)_{sample}/c_{sample}) \text{ X } (c_{BSA} \text{X } MM_{BSA} / I(0)_{BSA})$$

where c is the protein concentration. For the measurements BSA was prepared fresh in 20 mM Hepes, pH 8.0, 150 mM NaCl and 1 mM DTT at a concentration of ~5 mg/ml.

The pair distribution function which is proportional to the probability of observing a given distance inside the particle can be calculated using the indirect transform package GNOM (Svergun, 1992). The output of GNOM analysis is used in molecular shape modeling calculations. *Ab initio* calculations were carried out using the algorithms DAMMIN (Svergun, 1999) and GASBOR (Svergun et al., 2001). The models are calculated using dummy residues or beads by a simulated annealing procedure and the difference between the

scattering from the model and the experimental scattering intensity are minimized. Models were calculated using P2 symmetry since it was known from previous work that GSTdMT molecules dimerize at GST ends. Twelve different models were calculated with each algorithm and convergence of the models calculated by the two algorithms to a similar shape was observed. The final average model was obtained using DAMAVER (Volkov and Svergun, 2003).

4. RESULTS

4.1. G8C, G12C, G61C, G65C and G61CG65C Point Mutations and Sequence Verification

Cys motifs of the dMT sequence were modified by site-directed mutagenesis using the primers given in the Table 3.1. The cDNA and amino acid sequences of dMT gene and mutated regions are shown in Figure 4.1. The first step of site directed mutagenesis was monitored by verifying the existence of full length linear constructs using agarose gel electrophoresis. agarose .bands expected from the constructs at 5000 bp were observed after PCR reactions (Figure 4.2 A, B, C, D and E). Moreover, colonies were also checked for the presence of the genes by diagnostic digestion with restriction enzymes Eco*RI* and Xho*I* which had been engineered to the 5'- and 3'-ends of the *dmt* gene (Figure 4.3 A, B, C, D and E).

```
1   M   S   C   N   C   G   S   G   C   S   C   G   S   D   C   K   C   G   K   M    20
1   ATG TCT TGC AAC TGT GGA TCC GGT TGC AGC TGC GGC TCA GAC TGC AAG TGC GGG AAG ATG   60

    Y   P   D   L   T   E   Q   G   S   A   A   A   Q   V   A   A   V   V   V   L    40
61  TAC CCT GAT CTG ACA GAG CAG GGC AGC GCC GCC GCC CAG GTC GCC GCC GTG GTC GTG CTC  120

    G   V   A   P   E   N   K   A   G   Q   F   E   V   A   A   G   Q   S   G   E   60
121 GGC GTG GCT CCT GAG AAC AAG GCG GGG CAG TTC GAG GTG GCC GCC GGC CAG TCC GGC GAG 180

    G   C   S   C   G   D   N   C   K   C   N   P   C   N   C   *    75
181 GGC TGC AGC TGC GGC GAC AAC TGC AAG TGC AAC CCC TGC AAC TGT TAA  228
```

Figure 4.1: cDNA and amino acid sequences of dMT. C-X-C motifs (Grey) and regions which were mutated (Yellow) are highlighted. Single mutations were G8C, G12C, G61C and G65C. Double mutations were G8CG12C and G61CG65C.

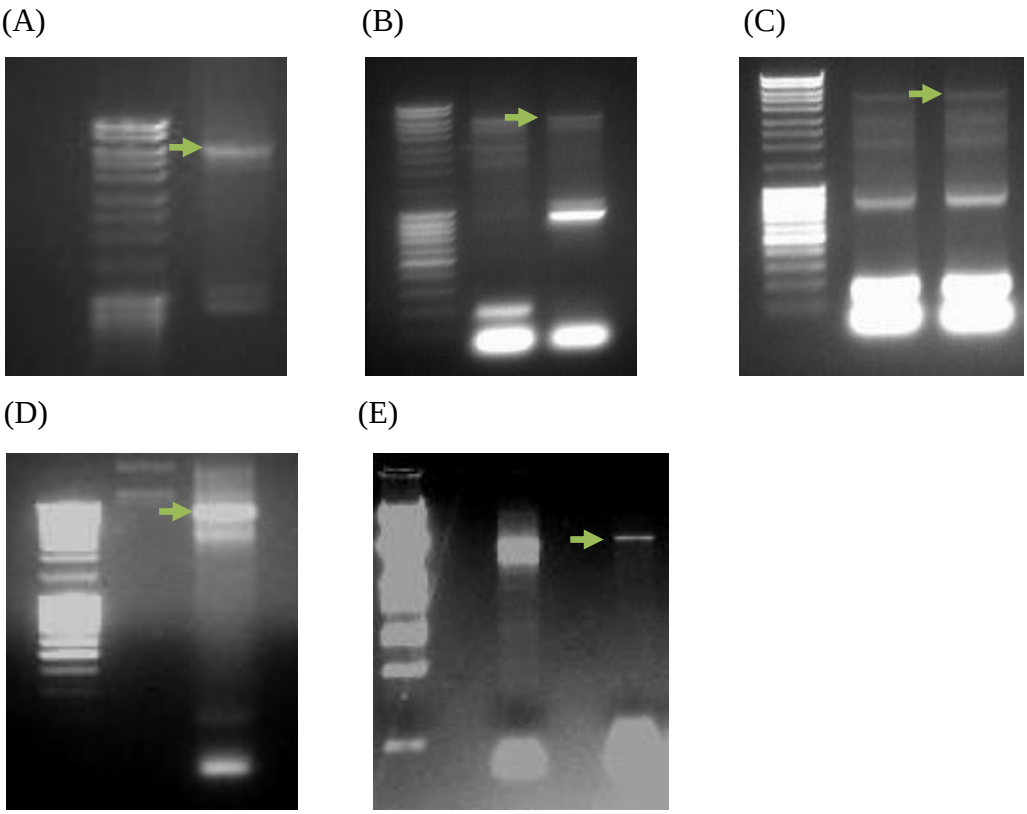

Figure 4.2: 1 % Agarose gel analysis of mutated GSTdMT constructs obtained by PCR. Lane 1: (A- E) Mass ruler DNA ladder mix. (A) Lane 2: G8C construct. (B) Lane 2: Control reaction. Lane 3: G12C construct. (C) Lane 2: Control reaction. Lane 3: G61C construct. (D) Lane 2: Control reaction. Lane 3: G65C construct. (E) Lane 2: Control reaction. Lane 3: G61CG65C construct. Arrows indicate the 5000 bp construct. Bands at the bottom of the gels are primers.

(A) (B) (C) (D) (E)

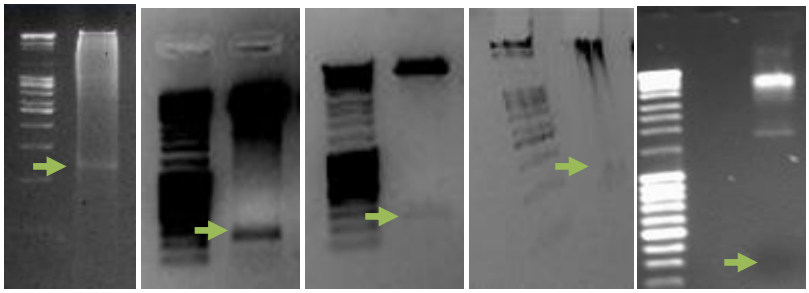

Figure 4.3: 1 % Agarose gel analysis of diagnostic digestion of positive colonies with *Eco*RI and *Xho*I. Lane 1: (A- E) Mass ruler DNA ladder mix. (A) Lane 2: G8C mutation (B) Lane 2: G12C mutation. (C) Lane 2: G61C mutation. (D) Lane 2: G65C mutation. (E) Lane 2: G61CG65C mutation. Arrows show the mutated fragment obtained after digestion.

Results of DNA sequencing to verify the mutations are given in Appendix B.

Attempts to obtain the double mutant G8CG12C were not successful. It has not been possible to detect by PCR the double mutant G8CG12C construct. Nevertheless, attempts were made to transform BL21DE3, Rosetta(DE3), Rosetta(DE3)plys5 cells with products from the first stages of SDM procedure. None of these attempts gave positive results.

4.2. Expression of Mutant G8C, G12C, G61C, G65C and G61CG65C Proteins in *E. Coli*

4.2.1.Monitoring the Growth of Transformed *E. coli* cells

E. coli BL21(DE3) cells were transformed with pGEX-4T-2-G8C, pGEX-4T-2-G12C, pGEX-4T-2-G61C, pGEX-4T-2-G65C and pGEX-4T-2-G61CG65C constructs and these cells and constructs will be refered as G8C, G12C, G61C, G65C and G61CG65C in the following text. Cell growth were monitored by measuring OD600 values before and after induction with 0.7 mM IPTG at regular intervals. Cells transformed with native empty vector, the GSTdMT construct and mutants were grown in LB medium with 0.1 mM $CdCl_2$. (Figure 4.4 A, B and C). Several growth curves were measured for G61CG65C construct and the absorbance values of cultures varied quite much. Hence, the variations in single mutated cells are ignorable. Growth curves of mutant cultures show similar growth for all constructs.

(A)

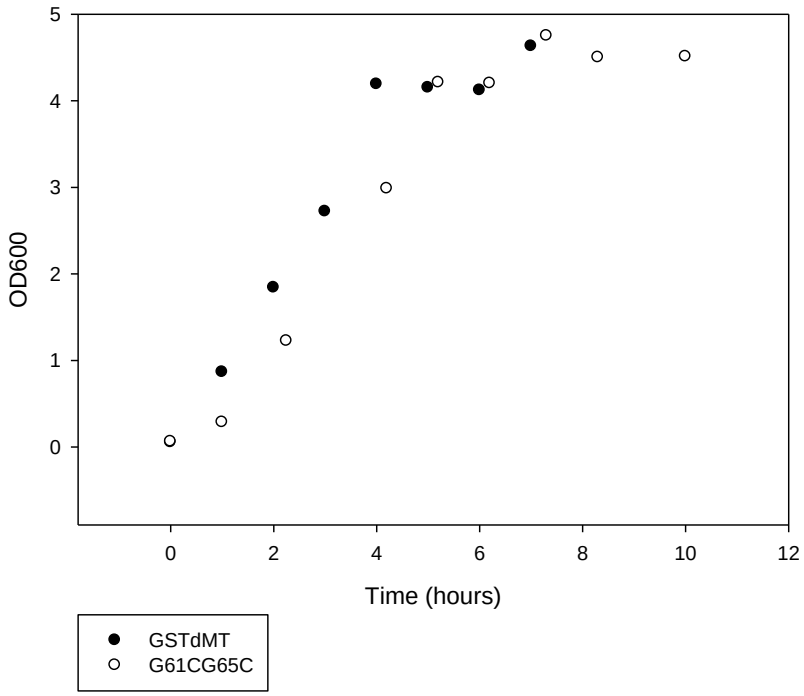
OD600
Time (hours)
GSTdMT
G61CG65C

(B)

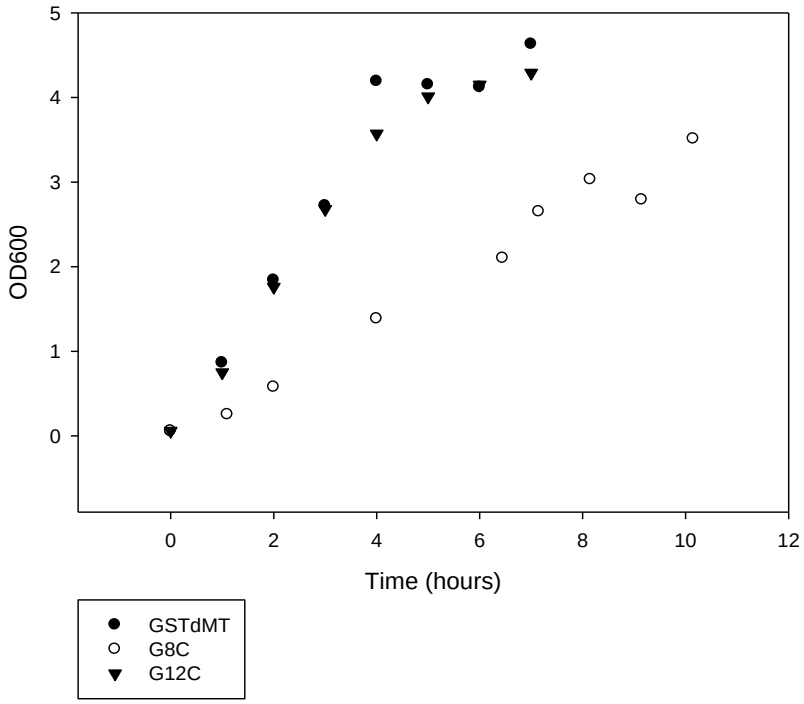
OD600
Time (hours)
GSTdMT
G8C
G12C

(C)

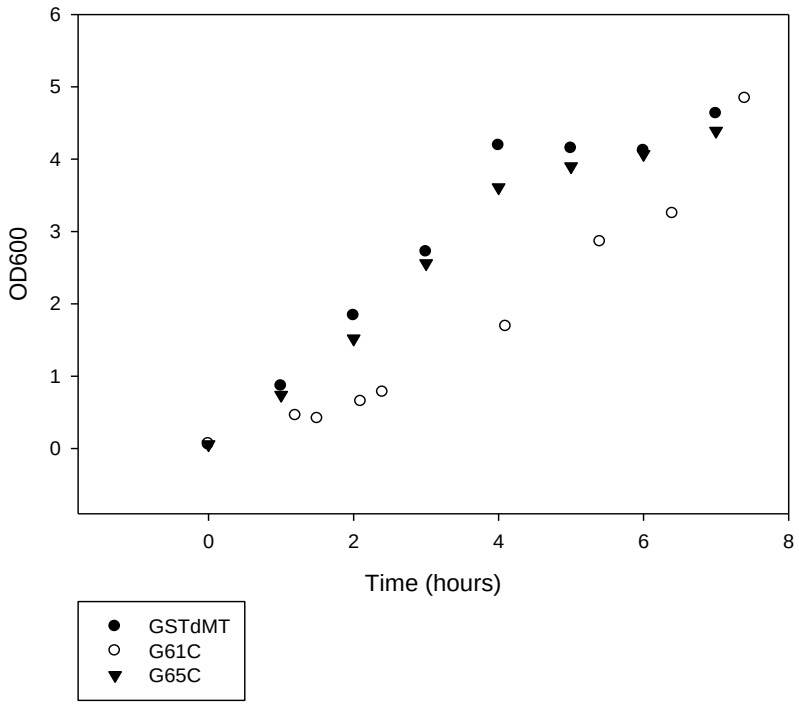

Figure 4.4: Comparative growth curves of 0.7 mM IPTG induced BL21(DE3) cells containing native GSTdMT vs. (A) G61CG65C (B) G8C and G12C (C) G61C and G65C constructs.

4.2.2.Monitoring the Expression of G61CG65C, G12 and G61

Expression of G61CG65C, G12 and G61 proteins were monitored by SDS-PAGE. In control experiments expression of GST (27 kDa) and native GSTdMT (35 kDa) were also monitored. Although the expression of the control proteins could be readily detected from analysis of cellular lysates on gels it has not been possible to visualize the mutants (Figure 4.5 A, B and C). Since the expression of the proteins cannot be checked from total cell lysate, this procedure was not followed for G8C and G65 mutants.

(A)

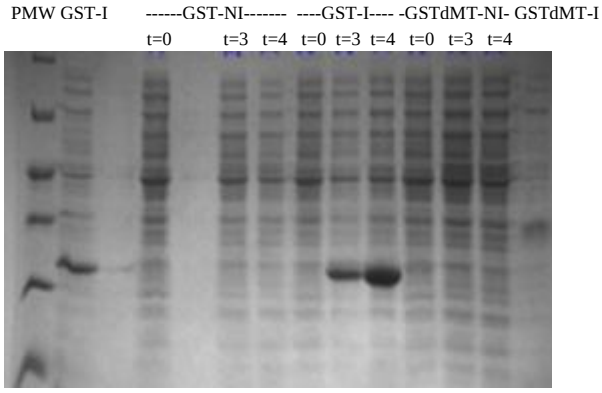

(B)

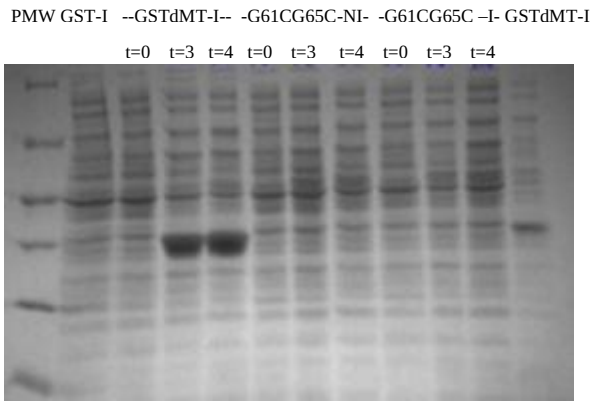

(C)

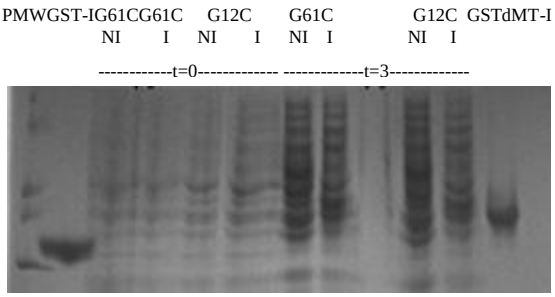

Figure 4.5: Time course of expression of (A) GST and GSTdMT (B) GSTdMT and G61CG65C (C) G12C and G65C monitored by 12 % SDS-PAGE. Samples and induction periods are indicated on the figure. *PMW: Unstained protein molecular weight marker. *NI: Non-induced. *I: Induced.

The expression of G61CG65C mutant was initially monitored by SDS-PAGE analysis of a batch purified sample and analytical scale. Cell lysates were incubated with GST affinity matrix and wash and elution fractions were analysed by SDS-PAGE. The mutant protein could not be observed in the soluble fraction (Figure 4.6). Further analyses were conducted to check if the protein was in the inclusion body fractions . However, these trials also did not give positive result (Not shown).

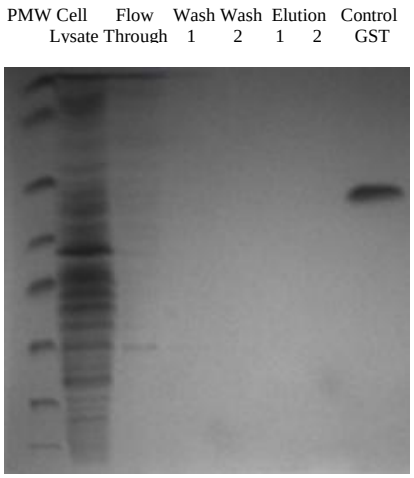

Figure 4.6: 12 % SDS-PAGE analysis of G61CG65C Batch Purification.

4.3. Purification of Mutants from *E. Coli*

The main purification and analysis procedure is summarized in Figure 4.6 (A and B). Cell lysates from 2.25 L bacterial cultures were loaded on the GSTrap FF column (GE Healthcare) and GST tagged proteins were eluted from the column with 20 mM reduced glutathione in Tris buffer (pH 8.0). Eluted fractions were pooled according to the protein content and dialysed overnight against Hepes buffer. Monodisperse protein was obtained by further fractionation using HiLoad 16/60 or 26/60 Superdex 75 size exclusion columns (GE Healthcare).

(A)

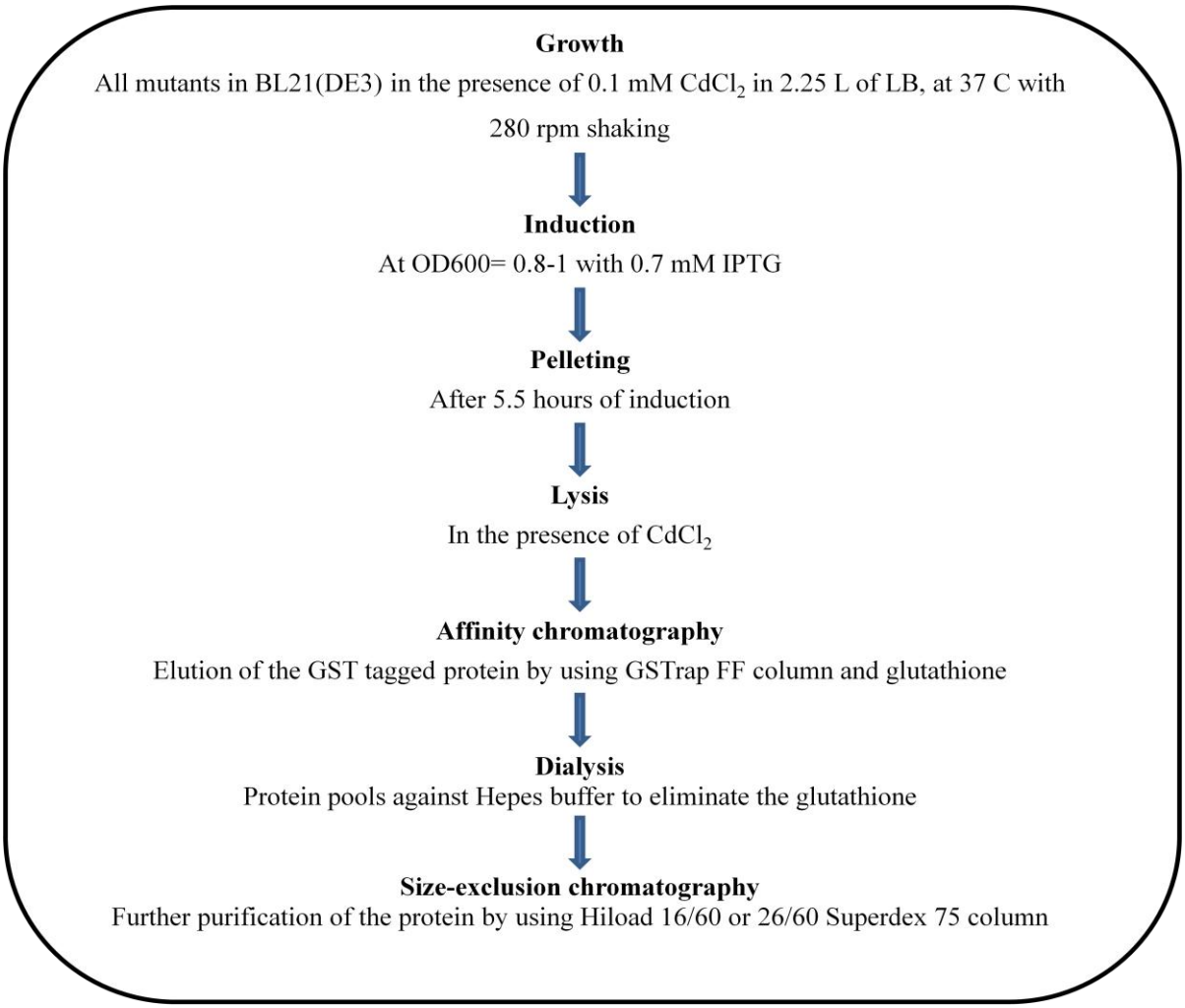
Growth
All mutants in BL21(DE3) in the presence of 0.1 mM $CdCl_2$ in 2.25 L of LB, at 37 C with 280 rpm shaking
Induction
At OD600= 0.8-1 with 0.7 mM IPTG
Pelleting
After 5.5 hours of induction
Lysis
In the presence of $CdCl_2$
Affinity chromatography
Elution of the GST tagged protein by using GSTrap FF column and glutathione
Dialysis
Protein pools against Hepes buffer to eliminate the glutathione
Size-exclusion chromatography
Further purification of the protein by using Hiload 16/60 or 26/60 Superdex 75 column

(B)

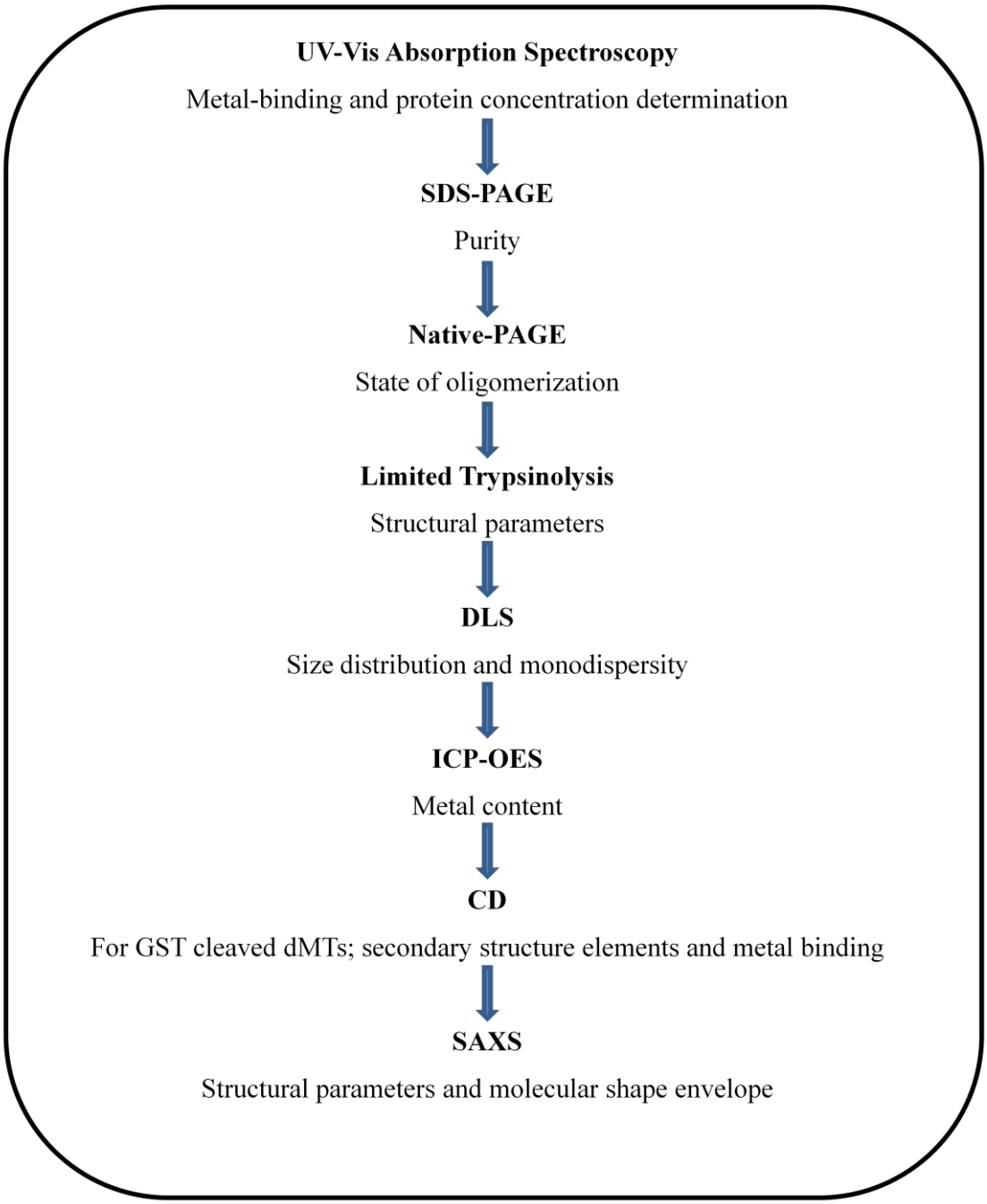

Figure 4.7: Schematic representation of (A) Purification procedure (B) Analyses steps

4.3.1. Affinity Chromatography

Mutant proteins were eluted from the GST affinity column with 10 mM reduced glutathione in Tris-HCl buffer (50 mM Tris-HCl, pH 8.0, 100 mM NaCl, 1 mM DTT, 0.5 mM PMSF, 1 tablet protease inhibitor cocktail). All fusion proteins showed similar elution patterns beginning at 2 ml (Figure 4.8 A, B, C and D). Peak fractions were pooled according to the A280 measurements. At this point of the procedure a total of about 25 mg fusion protein in 6 to 8 ml was obtained from 2.25 liters of culture.

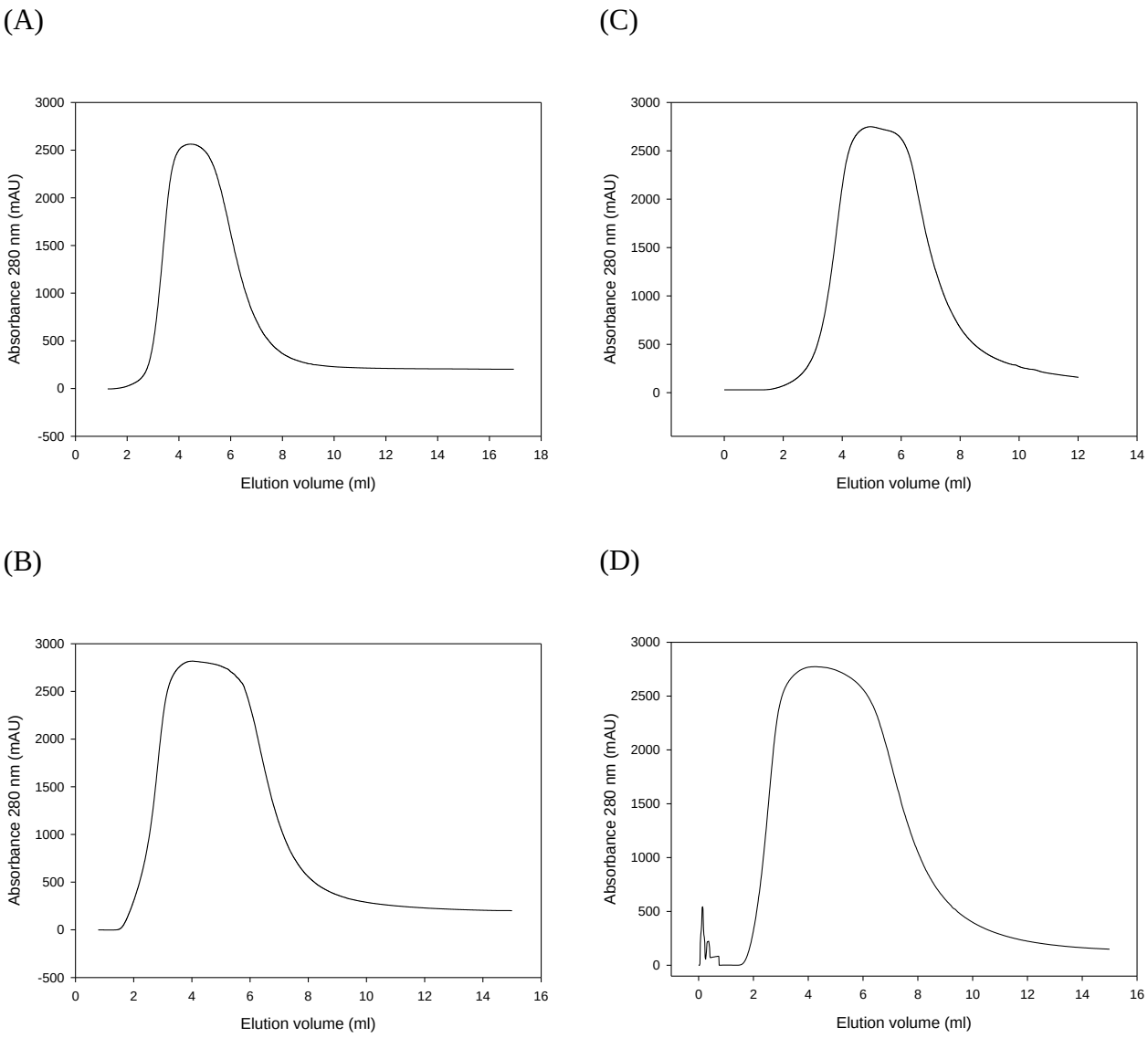

Figure 4.8: Elution profiles of (A) G8C (B) G12C (C) G61C (D) G65C from GSTrap FF affinity column.

4.3.2. Size Exclusion Chromatography

Two well resolved peaks were observed in the size exclusion chromatograms of the GSTdMT mutants. Peak 1 started to be eluted at around 49 ml and corresponded to aggregated forms. Peak 2 started to be eluted around 64 ml and represented the dimeric form (Figure 4.9 A, B, C and D). The major peak eluted at a position corresponds to about 70kDa.

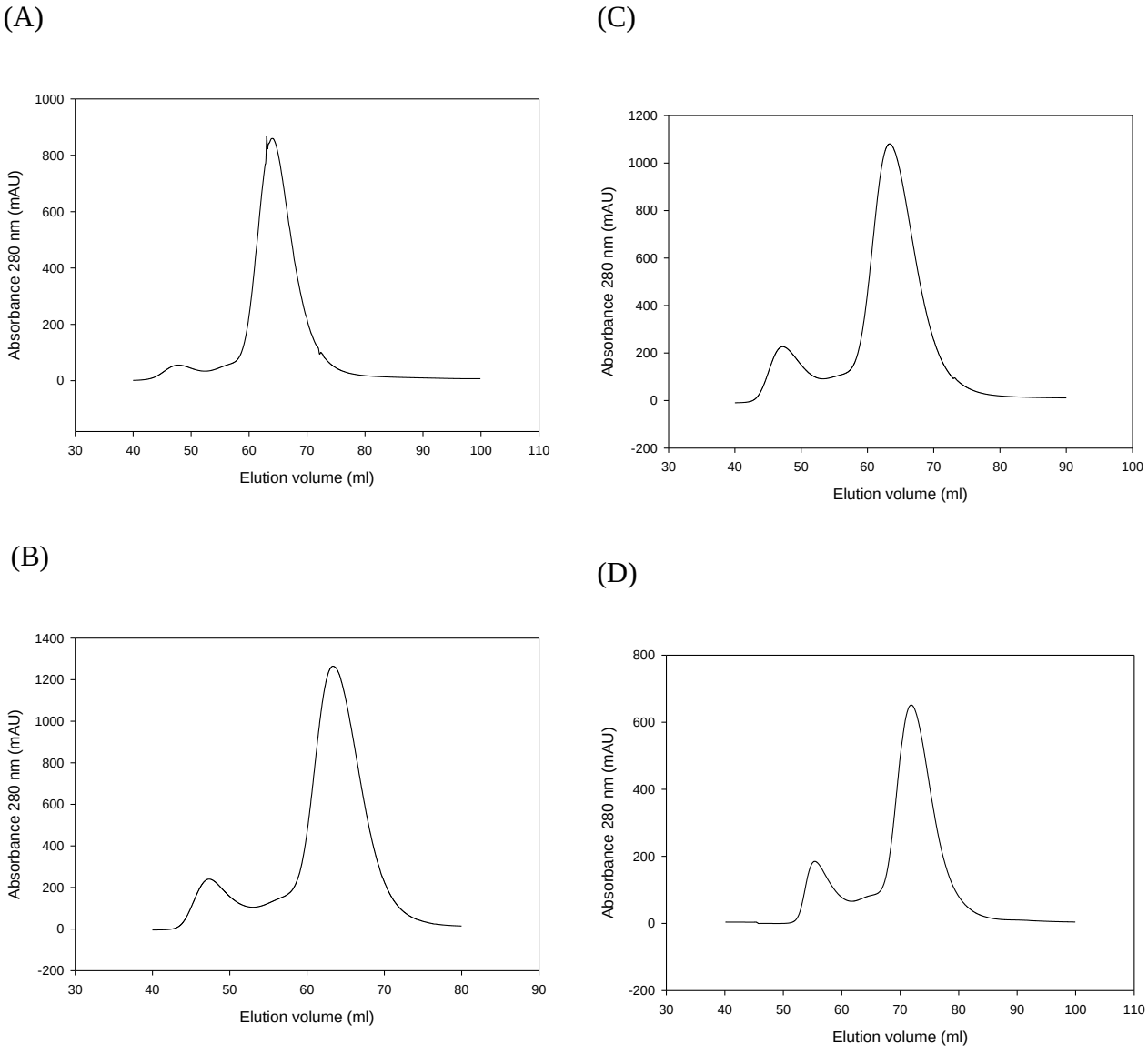

Figure 4.9: Elution profiles of (A) G8C (B) G12C (C) G61C (D) G65C from HiLoad 16/60 Superdex 75 size exclusion column.

4.4. Biochemical and Biophysical Analyses on the Mutant Proteins

4.4.1. SDS- and Native-PAGE Analyses

The pool from affinity chromatography and the fractions from size exclusion chromatography were analysed by 12 % SDS-PAGE to check for contaminants and protein degradation. Expected major band around 35 kDa was seen clearly with all mutants. In some cases, particuşarly after affinity chromatography, high and low molecular weight bands were also seen on the gels. High molecular weight bands indicated oligomeric species whereas low molecular weight bands are degradation products. After size exclusion chromatography less aggregation and degradation products were seen.

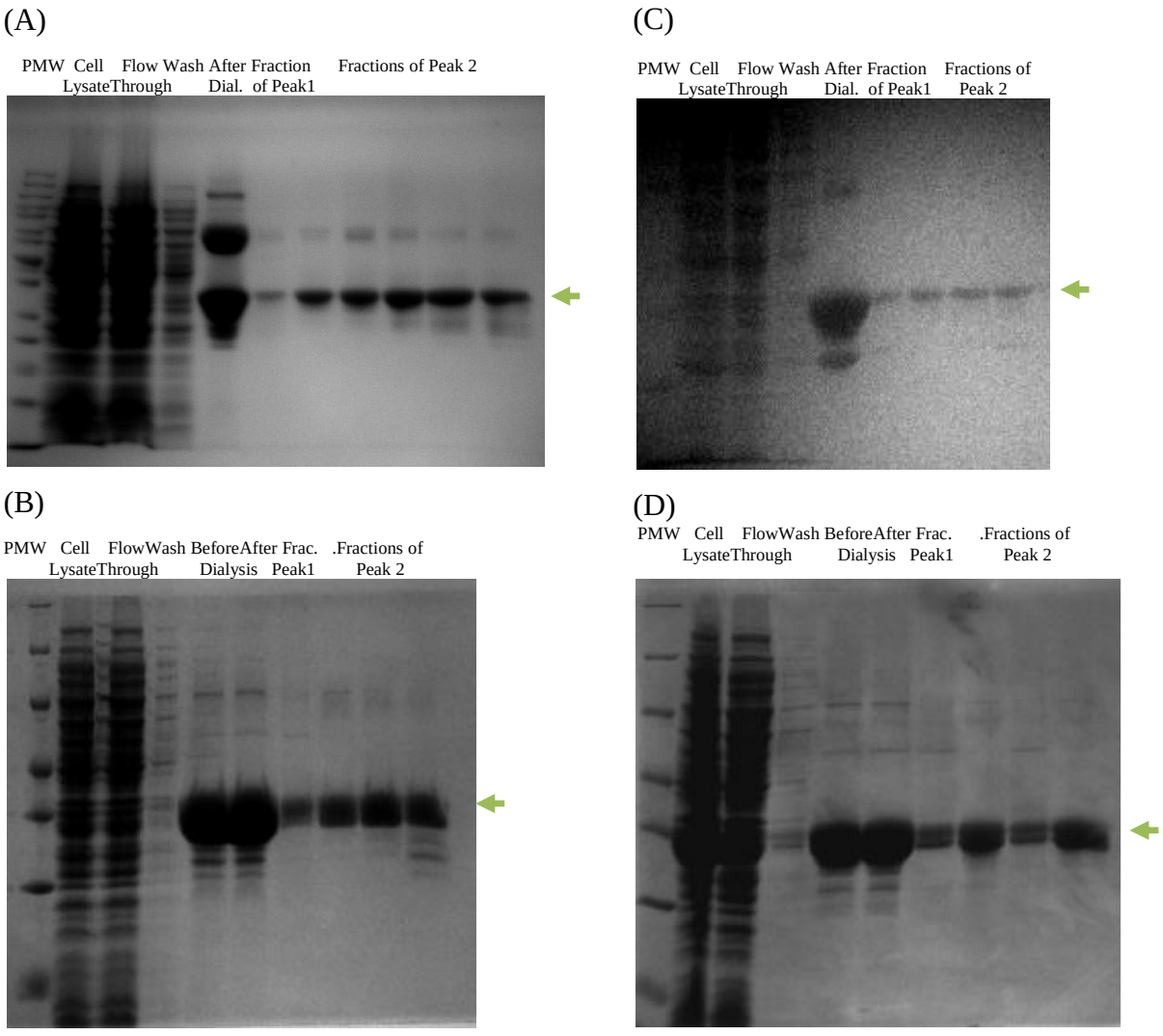

Figure 4.10: 12 % SDS-PAGE analysis of purified samples of (A) G8C (B) G12C (C) G61C (D) G65C. Arrows show the purified GSTdMT mutants.

The pool from affinity chromatography and the fractions from size exclusion chromatography were analysed by 8 % Native-PAGE as well. A major band corresponding to the protein and high molecular weight bands were corresponding to aggregates were present.

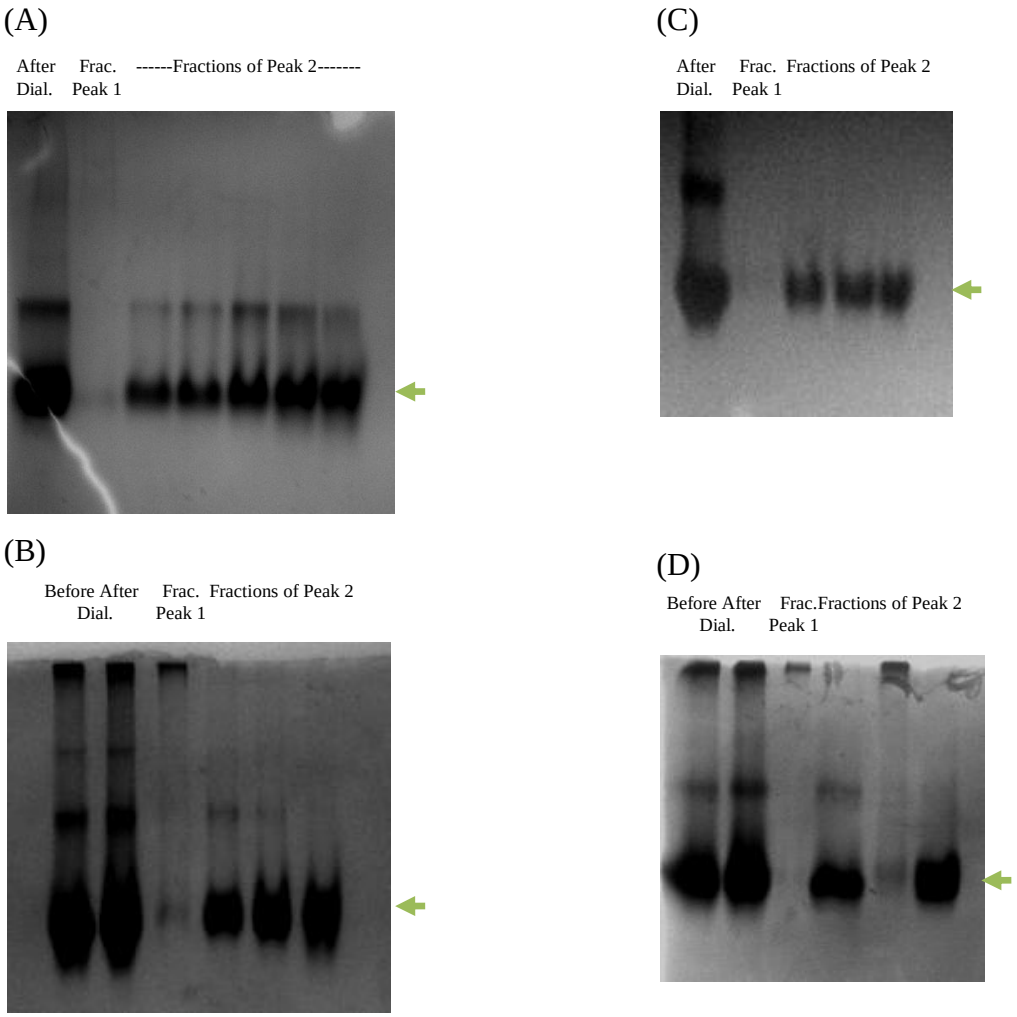

Figure 4.11: Native-PAGE analysis of purified samples of (A) G8C (B) G12C (C) G61C (D) G65C. Arrows show the purified GSTdMT mutants.

4.4.2. Limited Proteolytic Cleavage with Trypsin

Proteolytic cleavage of the GSTdMT mutants were performed with trypsin. Trypsin is a serine protease with a very well defined specificity. It cleaves peptides at the carboxyl side of lysine or arginine when either is followed by a proline. 16th, 19th, 47th and 69th lysine amino acids are the possible cleavage sites for dMT (Figure 4.12). Digestion results of GSTdMT mutants were analysed by 16 % Tris-tricine PAGE. As can be seen from the analyses in figure 4.13, in mutants G8C, G12C and G61C the band corresponding to GST appears within 30 seconds of exposure to the enzyme. The G65C mutant, however, shows a cleavage pattern which develops much slower than the others. GST band becomes significantly visible only after about 5 minutes.

GSTMSCNCGSGCSCGSDC**K**CG**K**MYPDLTEQGSAAAQVAAVVVLGVAPEN**K**AG QFEVAAGQSGEGCSCGDNC**K**CNPCNC

Figure 4.12: Amino acid sequence of dMT. Cleavage sites are (Red) highlighted.

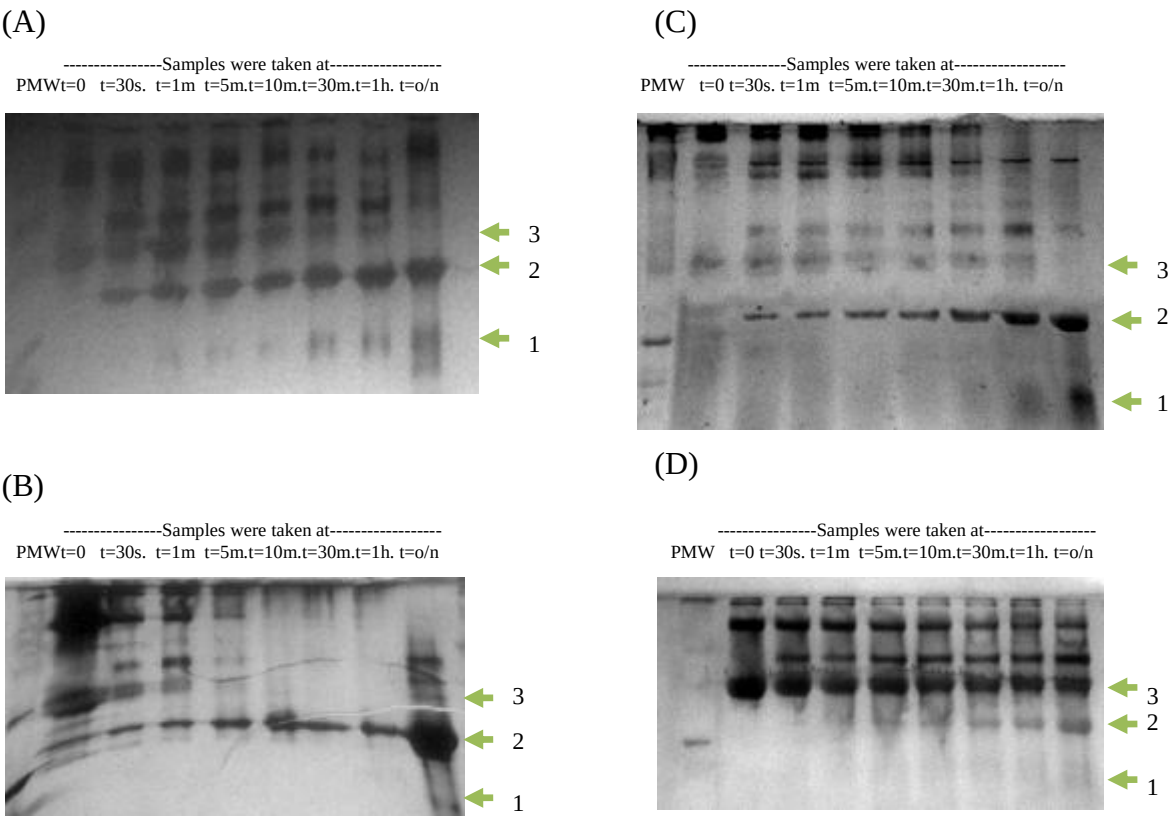

Figure 4. 13: 16 % Tris-tricine PAGE analysis of cleavage products of (A) G8C (B) G12C (C) G61C (D) G65C. While arrow1 shows dMT, arrow 2 shows GST and arrow 3 shows GSTdMT.

4.4.3. UV-Vis Spectrophotometric Characterization

GSTdMT have characteristic UV-Vis spectrum as a result of the absorption bands originating from the interaction of metal ions with the sulfur groups in the cystein rsidues. A peak at 280 nm is due to the aromatic residues in GST whereas between 240 and 260 nm a metal charge transfer band is seen due to the Cd-thiol interactions (Figure 4.14: A and B).

(A)

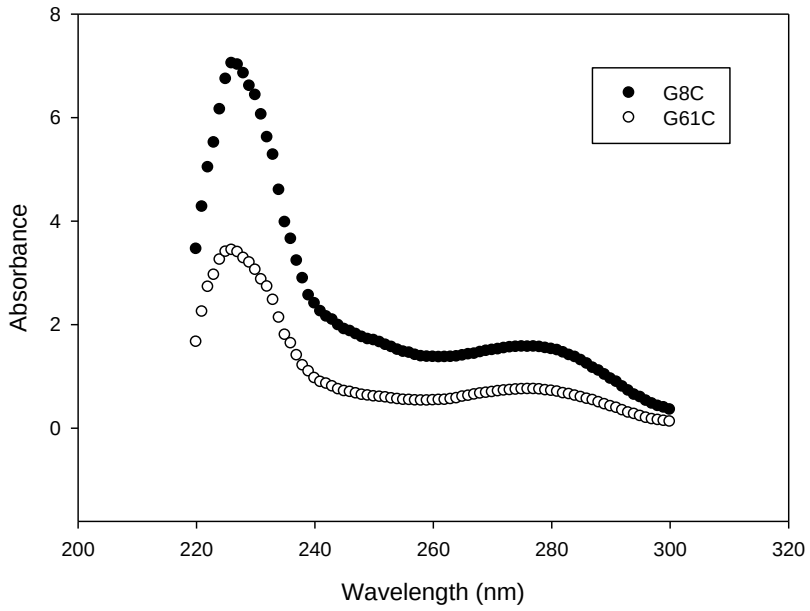

(B)

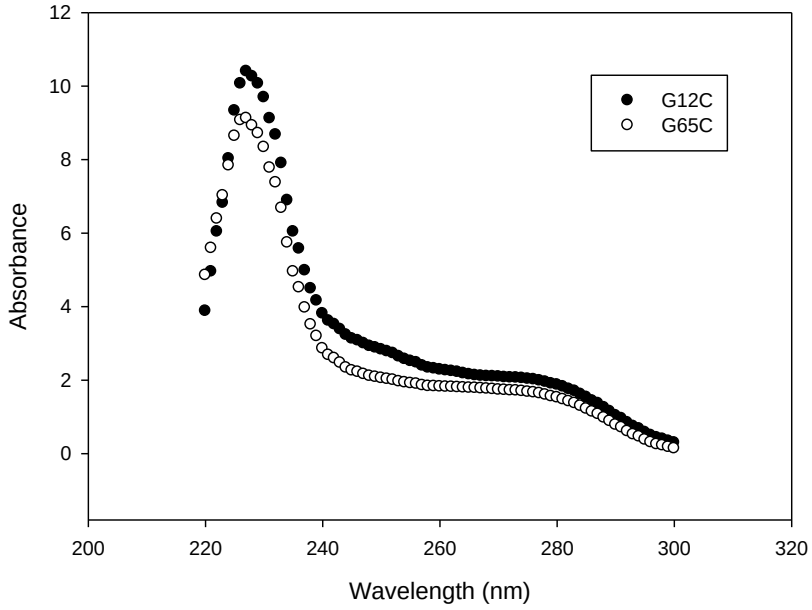

Figure 4. 14: Absorbance spectrum of (A) G8C and G61C, (B) G12C and G65C.

4.4.4. Dynamic Light Scattering (DLS)

Top fractions were analyzed by DLS to monitor the degree of oligomerization and monodispersity of the samples.

According to the size distribution by intensity only a small amount of aggregates existed in the fractions. These oligomeric forms have diameter of about 300 nm in all cases. As seen all intensity graphs. Moreover, a single peak in intensity distribution of the scattered light indicates that the mutant protein solutions are monodisperse. Moreover, hydrodynamic radius of the dominant particle is around 10 nm.

(A)

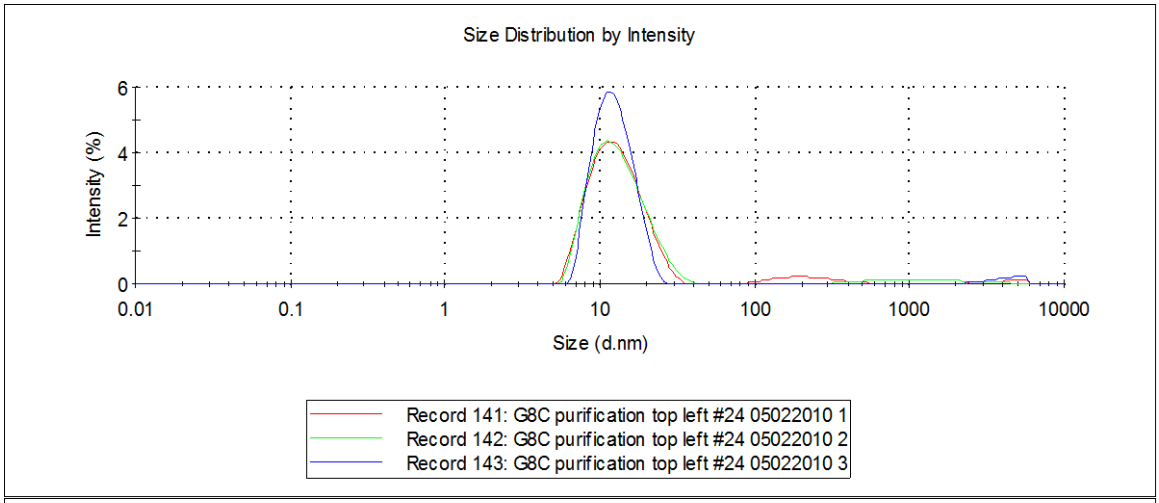
Size Distribution by Intensity
Intensity (%)
0
2
4
6
0.01
0.1
1
10
100
1000
10000
Size (d.nm)
Record 141: G8C purification top left #24 05022010 1
Record 142: G8C purification top left #24 05022010 2
Record 143: G8C purification top left #24 05022010 3

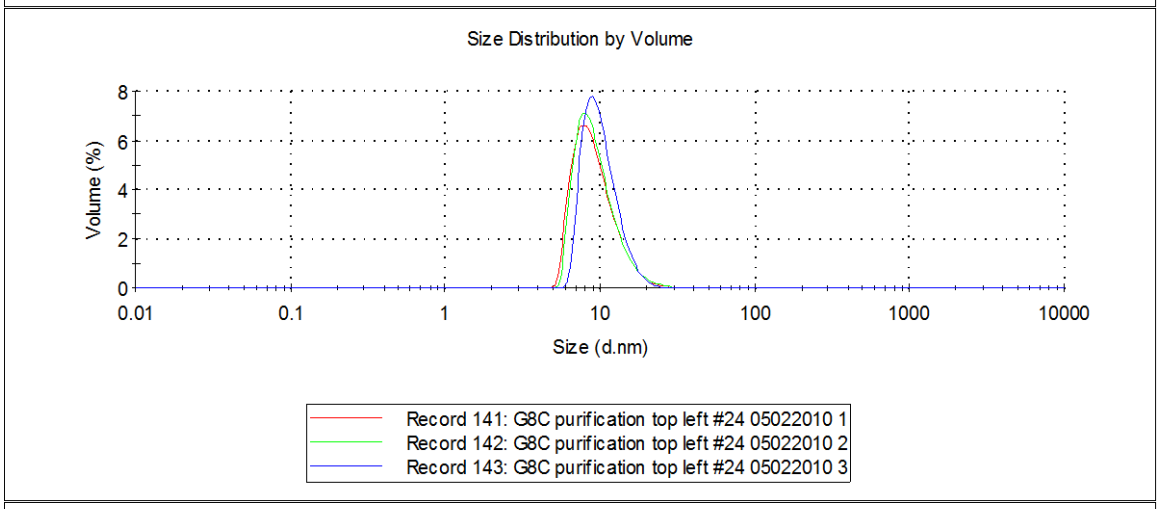
Size Distribution by Volume
Volume (%)
0
2
4
6
8
0.01
0.1
1
10
100
1000
10000
Size (d.nm)
Record 141: G8C purification top left #24 05022010 1
Record 142: G8C purification top left #24 05022010 2
Record 143: G8C purification top left #24 05022010 3

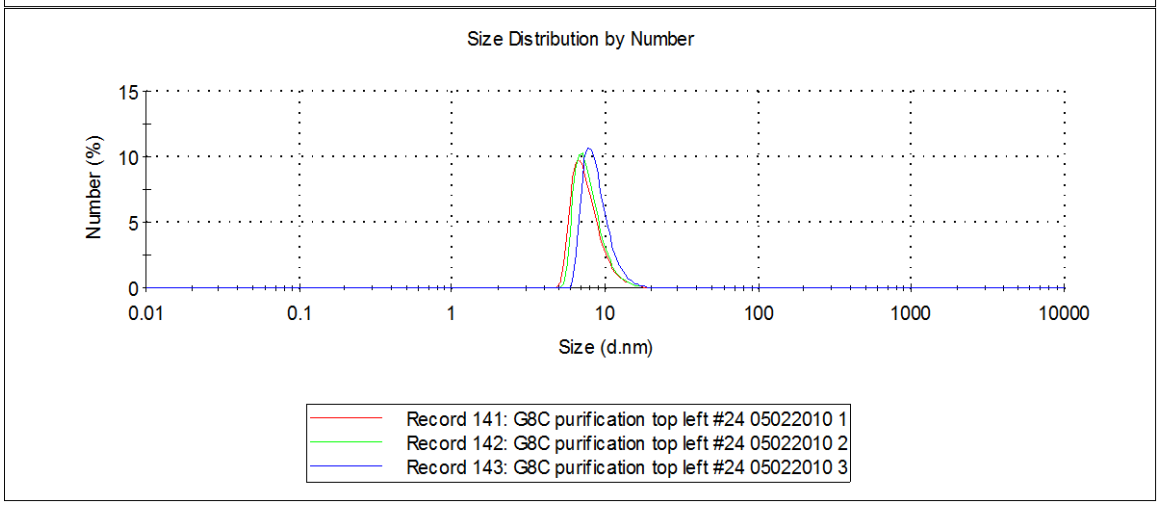
Size Distribution by Number
Number (%)
0
5
10
15
0.01
0.1
1
10
100
1000
10000
Size (d.nm)
Record 141: G8C purification top left #24 05022010 1
Record 142: G8C purification top left #24 05022010 2
Record 143: G8C purification top left #24 05022010 3

(B)

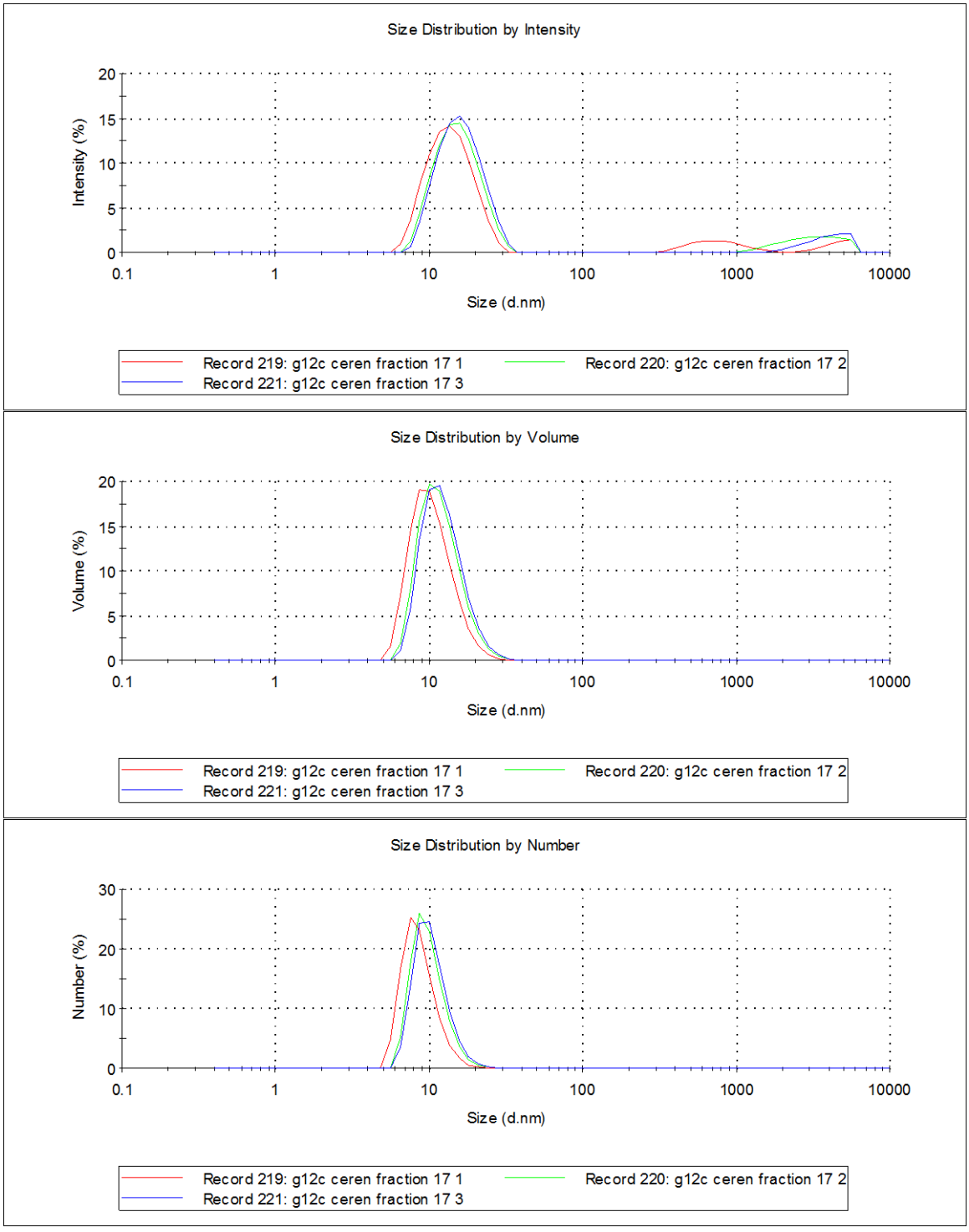
Size Distribution by Intensity
Intensity (%)
20
15
10
5
0
0.1
1
10
100
1000
10000
Size (d.nm)
Record 219: g12c ceren fraction 17 1
Record 220: g12c ceren fraction 17 2
Record 221: g12c ceren fraction 17 3
Size Distribution by Volume
Volume (%)
20
15
10
5
0
0.1
1
10
100
1000
10000
Size (d.nm)
Record 219: g12c ceren fraction 17 1
Record 220: g12c ceren fraction 17 2
Record 221: g12c ceren fraction 17 3
Size Distribution by Number
Number (%)
30
20
10
0
0.1
1
10
100
1000
10000
Size (d.nm)
Record 219: g12c ceren fraction 17 1
Record 220: g12c ceren fraction 17 2
Record 221: g12c ceren fraction 17 3

(C)

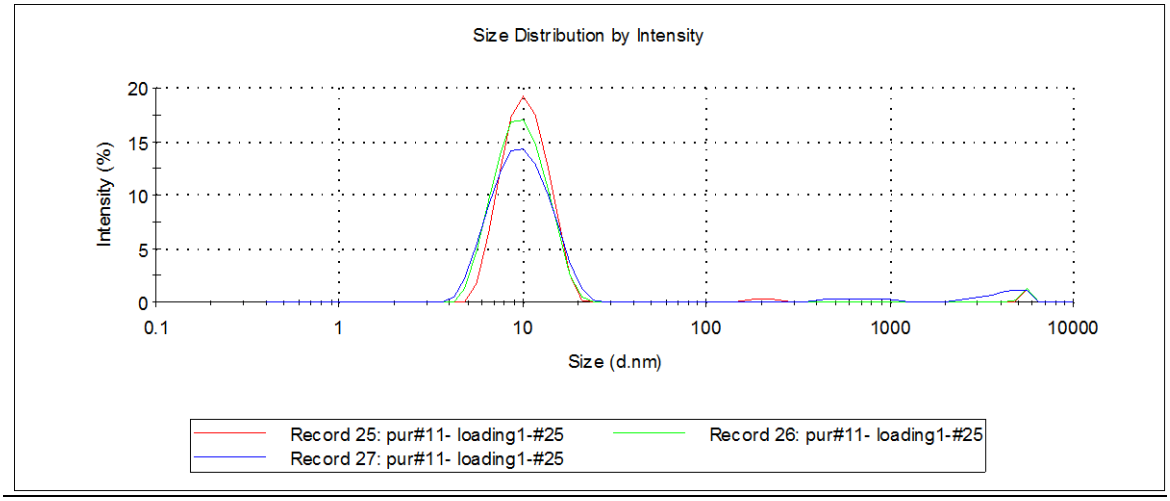
Size Distribution by Intensity
Intensity (%)
20
15
10
5
0
0.1
1
10
100
1000
10000
Size (d.nm)
Record 25: pur#11- loading1-#25
Record 26: pur#11- loading1-#25
Record 27: pur#11- loading1-#25

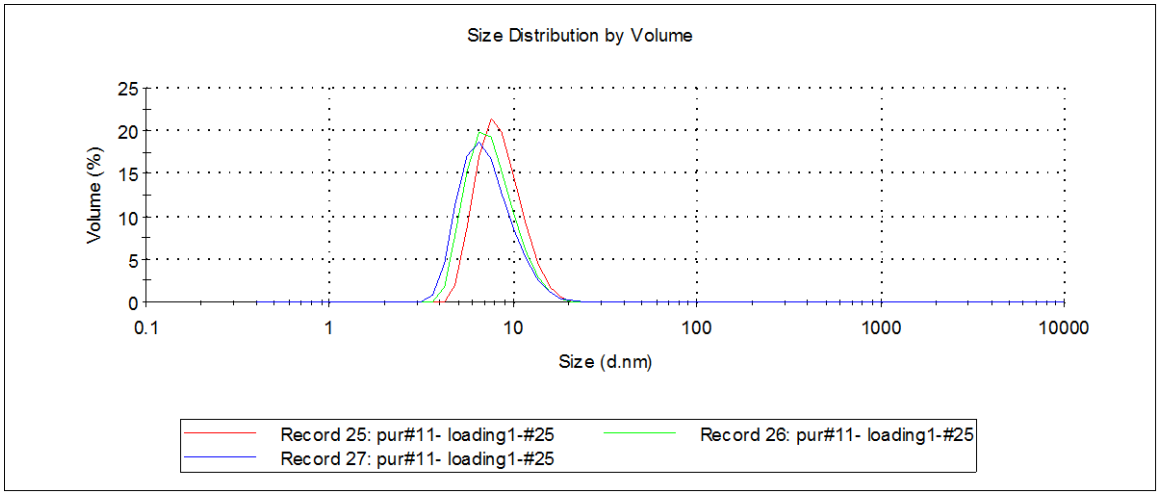
Size Distribution by Volume
Volume (%)
25
20
15
10
5
0
0.1
1
10
100
1000
10000
Size (d.nm)
Record 25: pur#11- loading1-#25
Record 26: pur#11- loading1-#25
Record 27: pur#11- loading1-#25

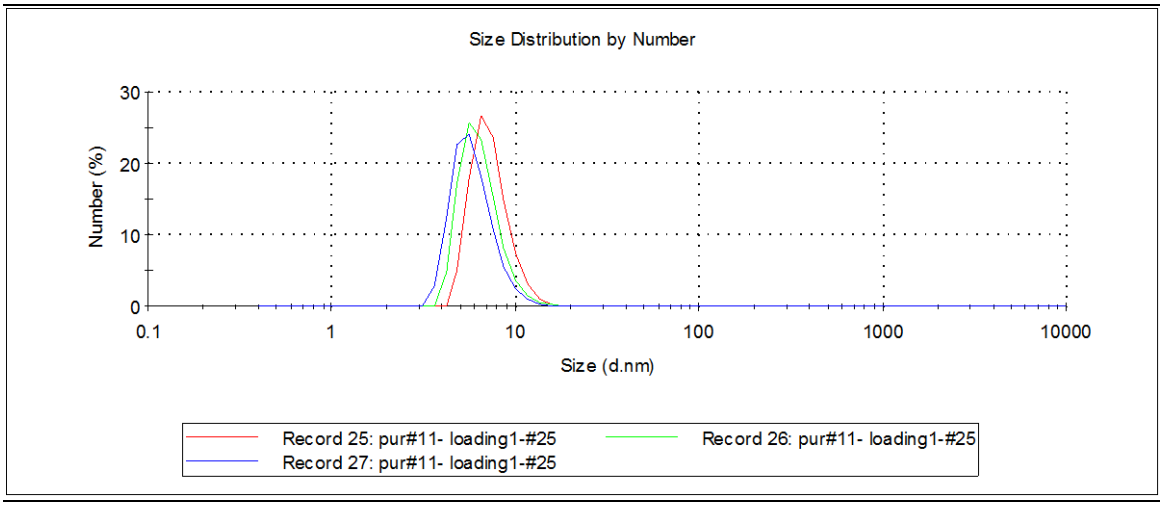
Size Distribution by Number
Number (%)
30
20
10
0
0.1
1
10
100
1000
10000
Size (d.nm)
Record 25: pur#11- loading1-#25
Record 26: pur#11- loading1-#25
Record 27: pur#11- loading1-#25

(D)

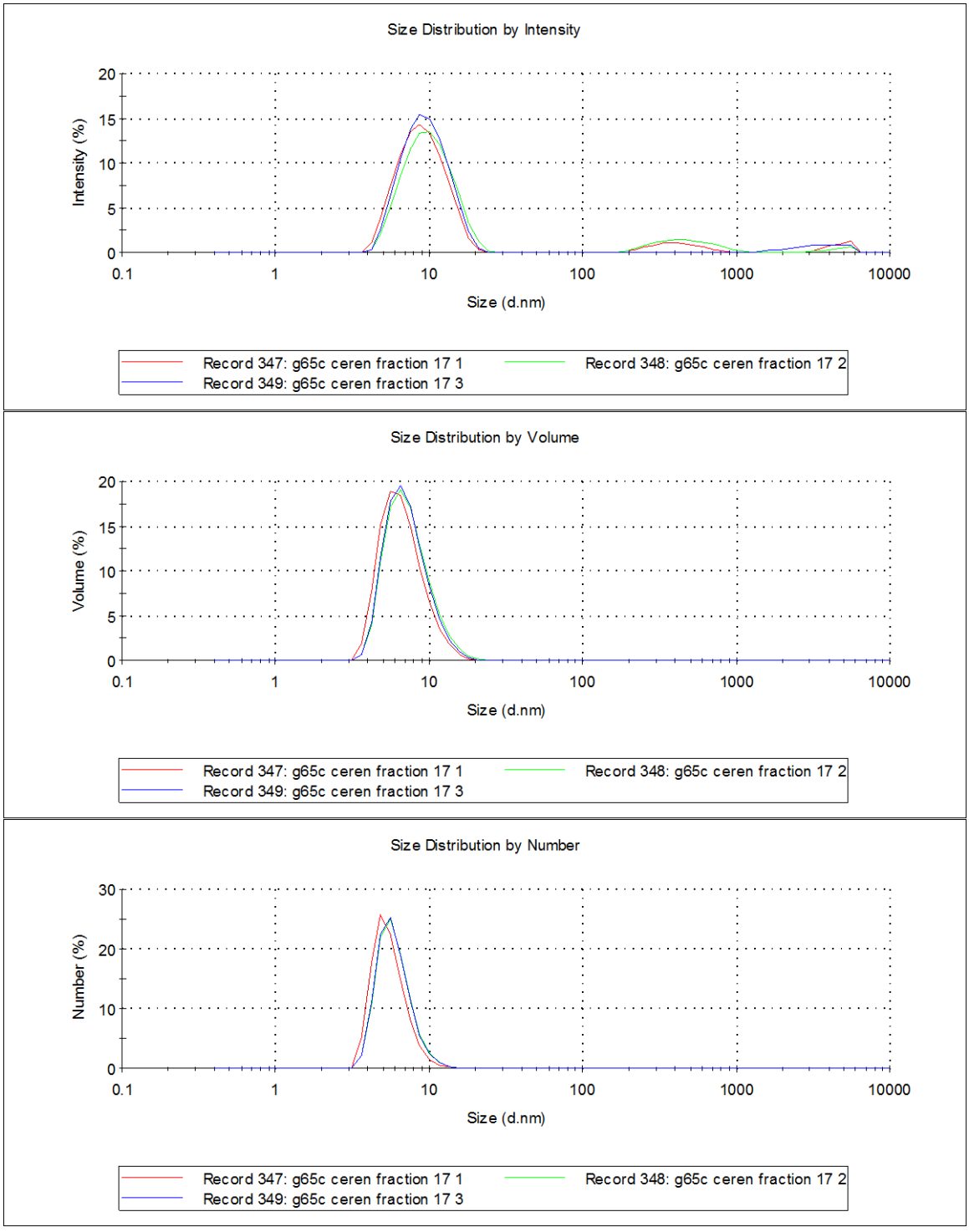

Figure 4.15: Dynamic light scattering (DLS) measurements of purified (A) G8C (B) G12C (C) G61C (D) G65C.

4.4.5. Thrombin cleavage of G65C

First a small scale cleavage was done to determine if G65C can be cleaved from GST by thrombin. Approximately 0.3 mg of purified protein protein was incubated with 3U of thrombin in the cold room. Samples were taken before and after overnight incubation, the cleaved protein was analysed by 16 % Tris tricine gel. GST (27 kDa) and dMT (7 kDa) bands are seen clearly (Figure 4.16).

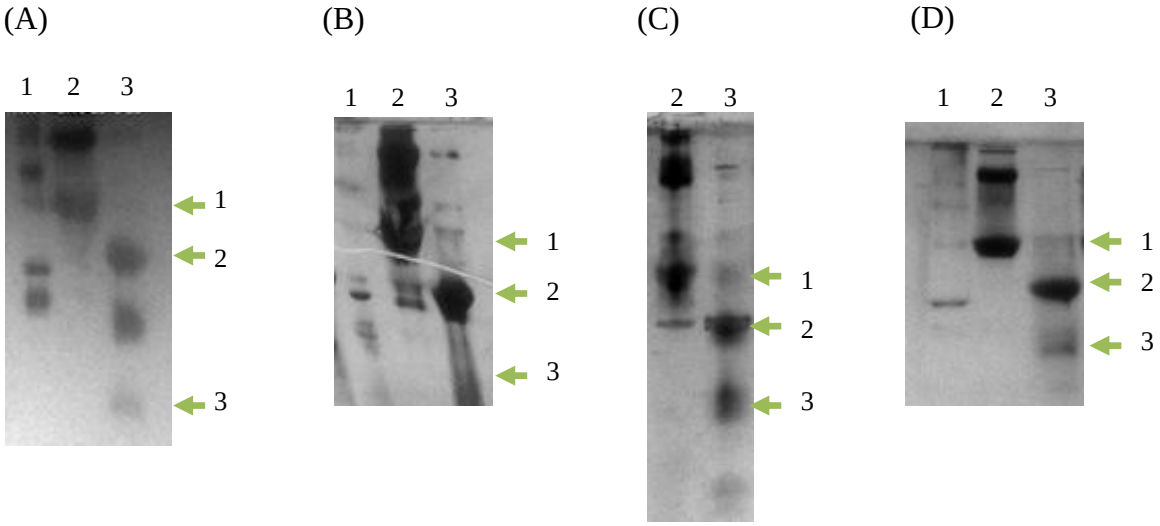

Figure 4.16: 16 % Tris-tricine PAGE analysis of thrombin cleavage of (A) G8C (B) G12C (C) G61C (D) G65C. Lane 1: Protein molecular weight marker. Lane 2: Undigested GSTdMT mutant. Lane 3: mutants cleaved from GST with thrombin o/n incubation with thrombin. While arrow1 shows GSTdMT, arrow 2 shows GST and arrow 3 shows dMT.

Large scale purification of G65C was carried out from 3 liter cultures to characterize the mutant protein. Affinity purified protein was loaded on a Hiload 16/60 Superdex 75 column after 16 hours of thrombin cleavage. Cleaved dMT started to be eluted from at 80 ml.

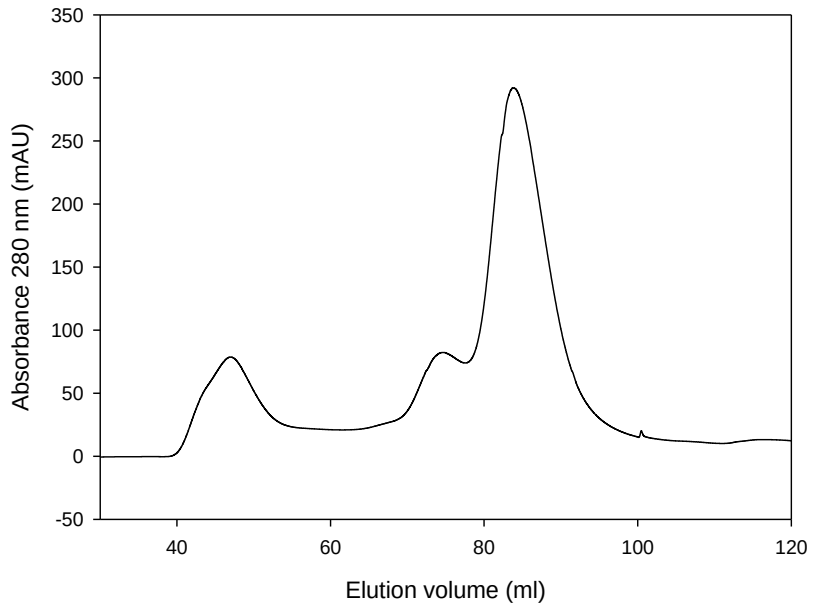

Figure 4.17: Elution profile of G65C on Hiload 16/60 Superdex 75 size exclusion column.

4.4.6. Circular Dichroism Spectropolarimetry (CD) of G61C

CD spectropolarimetry was used to characterize the secondary and tertiary structures. Since Hepes buffer have an absorbance in far-UV region of the spectrum, it is substracted to eliminate noisy data.

In the CD spectrum of G61C mutant (Figure 4.18), a peak around 240 nm, related to Cd-S interactions, is observed. In the far UV region the minimum around 200 nm points to a random coil dominated structure.

This result is in agreement with the CD pattern of the native dMT (Yesilirmak, 2008).

Data pitch	0.05
Band width (nm)	1
Response (sec)	4
Sensitivity	standard
Range (nm)	200-300
Speed (nm/min)	50
Accumulations	3
Path length (mm)	1
Temp. (^{o}C)	26

Table 4.1: Conditions in which the measurements were performed.

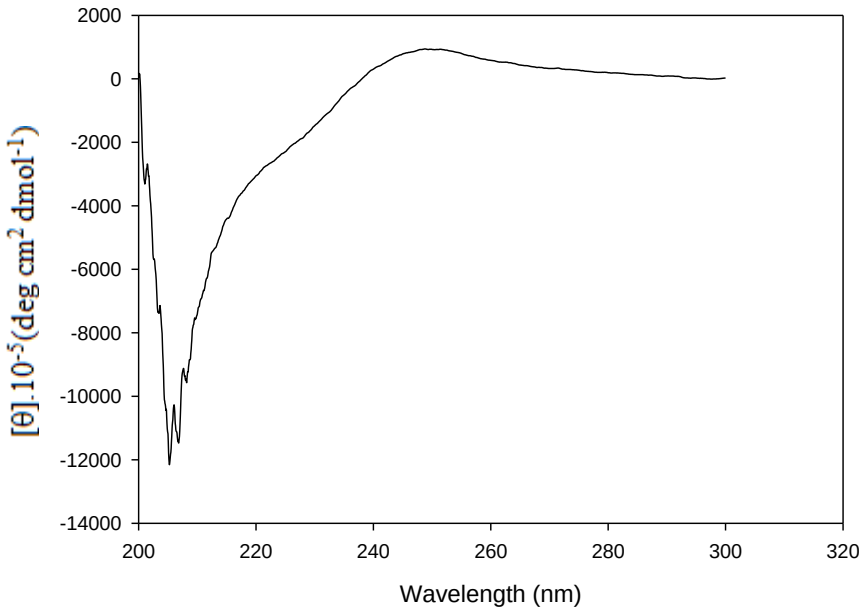

Figure 4.18: CD Spectra of G61C

4.4.7. Cd^{2+} content of mutant proteins:

Cd2+/protein ratio for the mutants were measured by Inductively Coupled Plasma Optical Emission Spectroscopy (ICP-OES). Several samples from the same purification were analysed by ICP-OES. Reproducibility of the results was shown by comparing different purifications on the same mutant. Results shown on table 4.2 were calculated using protein concentrations calculated from A_{280} absorbance values and bound Cd^{2+} was measured by ICP-OES to determine the binding ratio of Cd^{2+}.

	Cd^{2+} Molarity(μM)	Protein Molarity (μM)	Cd^{2+}/Protein ratio
G8C	0.0000882±0.0000674	0.0000241±0.0000179	3.61±0.36
G12C	0.0001831±0.0000708	0.0000517±0.0000172	3.46±0.45
G61C	0.0001370±0.0001910	0.0000372±0.0000475	3.54±0.61
G65C	0.0001280±0.0000356	0.0000295±0.0000085	4.36±0.46

Table 4.2: Cd^{2+}/Protein ratio for G8C, G12C, G61C and G65C mutants.

According to analysis of results from different purifications, the average Cd^{2+}/Protein ratio of G8C, G12C and G61C mutants are 3.5, similar to native GSTdMT when expressed in the presence of 0.1 mM $CdCl_2$. But, G65C mutation enhances Cd binding. This mutant binds 4.5 Cd/protein as compared to 3.5 Cd/protein by native GSTdMT and the other mutants.

4.4.8. Structural Characterization of G61C Using Small Angle X-Ray Scattering (SAXS)

Small angle solution X-ray scattering measurements were carried out using the mutant protein G61C to determine structural parameters and shape of the molecule for comparison with native GSTdMT. Measurements were carried out only on this mutant because of the limited availability of beamtime at the synchrotron.

The SAXS profile shown in Figure 4.19 was collected from a protein sample at 6.5 mg/ml in HEPES buffer. The structural parameters obtained using this data and the Guinier plot shown in Figure 4.20 are given in Table 4.3. As can be seen from the experimental value of the molecular weight given in Table 4.3 and consistent with earlier results on native GSTdMT (Bilecen et al., 2005, Yesilirmak, 2008), G61C mutant forms dimers in solution. The experimentally determined molecular mass of 78 kD agrees with the theoretical value of 68 within the error margin of measurements. Calculations of the molecular shape by indirect transform GNOM has resulted in the pair distribution function shown in Figure 4.21 (A) and the agreement between the scattering from the calculated shape and the experimental data is shown in Figure 4.21 (B). The shape of the pair distribution function indicates that the protein in solution has an extended shape. The maximum particle dimension is 11.6 nm. The parameters obtained from GNOM analysis are given in Table 4.4. There is good agreement between these parameters and those obtained directly from the experimental data.

Low resolution molecular shape envelopes for the G61C mutant calculated using Dammin and Gasbor algorithms are shown in Figure 4.22 and 4.23 (A) and (B). As indicated by the pair distribution function the dimer has a central domain where the GST molecules are located and the dMT molecules extend from this central domain in opposite direction without making contact with each other.

Sample	Data Limits	sRg Limits	Rg (nm)	I(0)	MM_{th} (kD)	MM_{exp} (kD)
G61C (6.5 mg/ml)	80-118	0.953<sRg<1.288	3.31±0.14	103.47	68.07	78

Table 4.3: Structural parameters of G61C obtained from SAXS data.

Rg: radius of gyration, s: momentum transfer, I(0) scattering intensity at s = 0, MM_{th}: theoretical value of the molecular mass of the dimer obtained from the amino acid sequence. MM_{exp}: molecular mass determined from I(0).

Sample	Data Limits	Dmax (nm)	Rg (nm)	I(0)	MM_{th} (kD)	MM_{exp} (kD)
G61C (6.5 mg/ml)	80-1000	11.6	3.43	104	68.070	52

Table 4.4: Structural parameters of G61C obtained from GNOM analysis.

Rg: radius of gyration, I(0) scattering intensity at s = 0, MM_{th}: theoretical value of the molecular mass of the dimer obtained from the amino acid sequence. MM_{exp}: molecular mass determined from I(0).

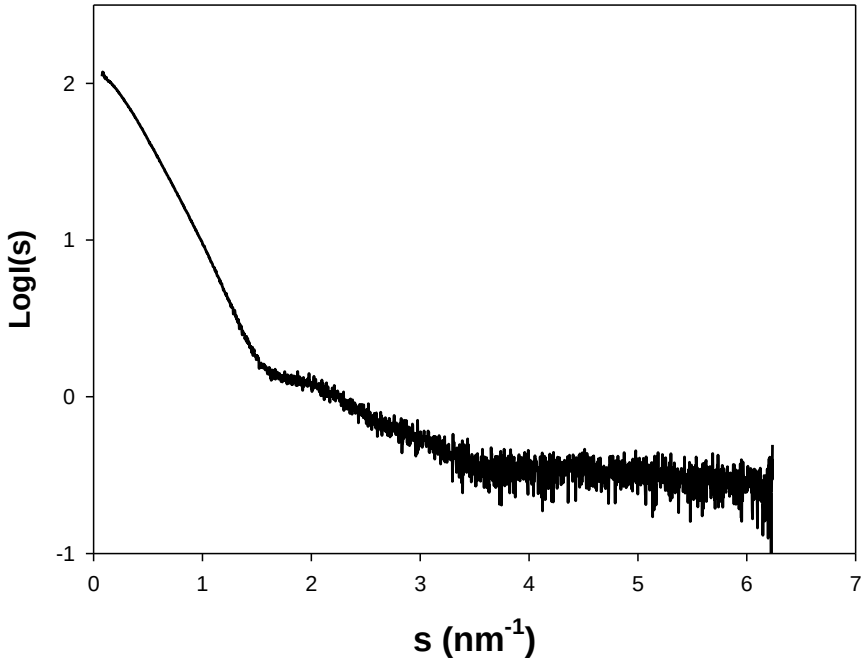

Figure 4.19: SAXS curve from G61C mutant. I(s) is the scattered intensity and s is the momentum transfer.

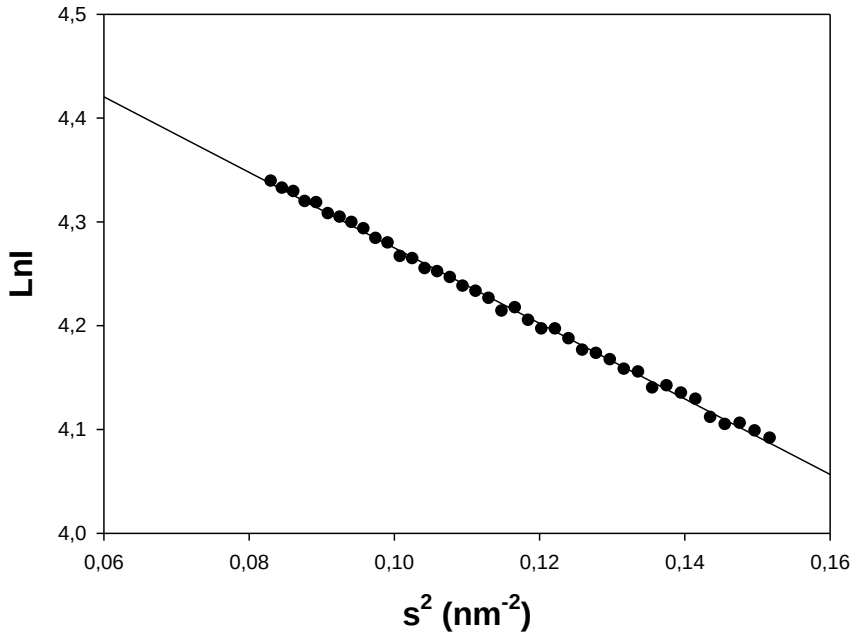

Figure 4.20: Guinier plot for G61C mutant obtained from the SAXS curve shown in Figure 4.19.

(A)

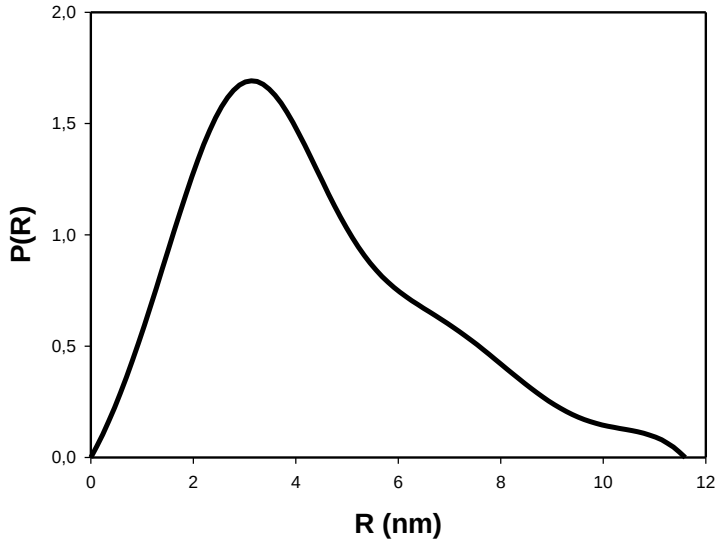

(B)

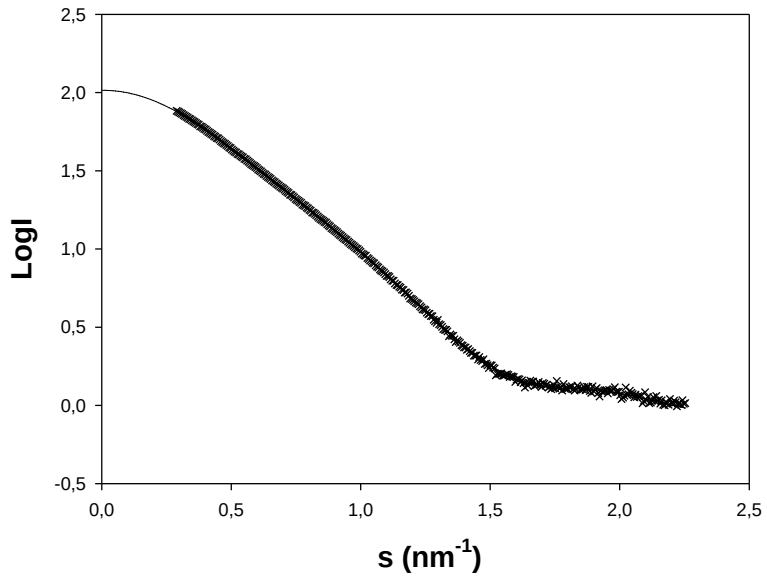

Figure 4.21: GNOM indirect transform analysis of the SAXS data for the G61C mutant.(A) Pair distribution function P(R). (B) Comparison of the scattering intensity calculated from the transform (—) with the experimental data (X) .

(A)

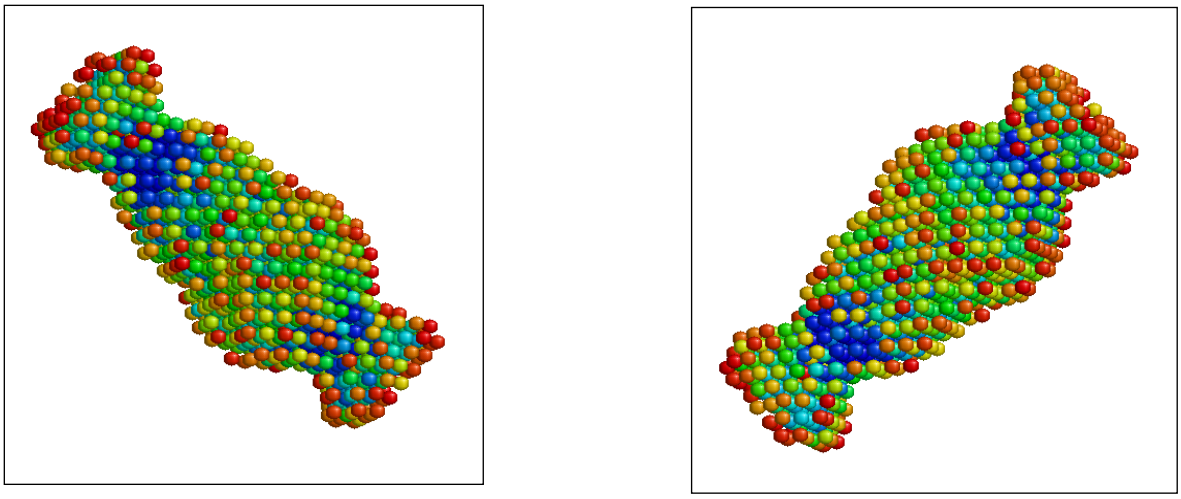

(B)

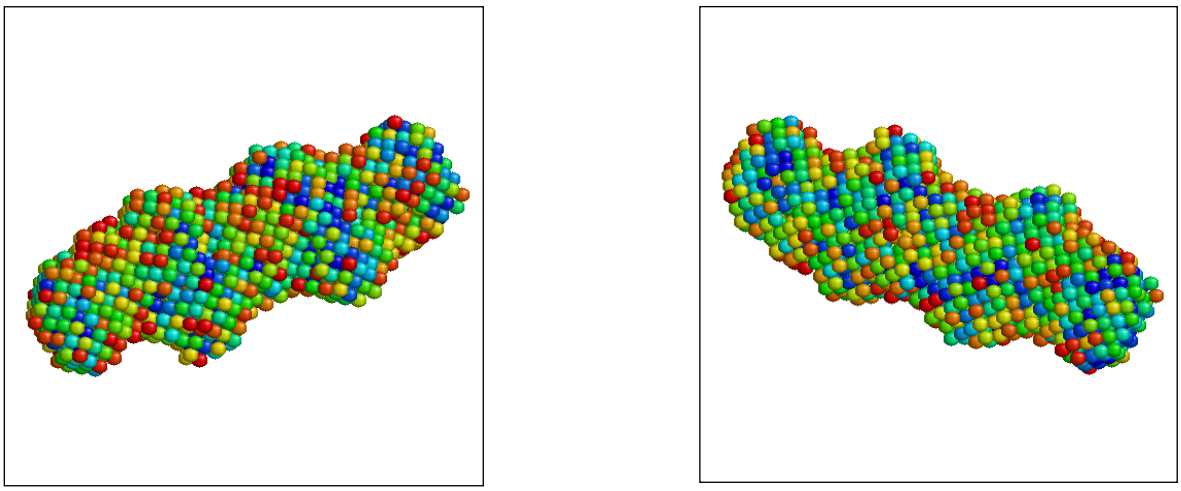

Figure 4.22: Low resolution *ab initio* shape models for G61C. (A) Models obtainded by Dammin algorithm. (B) Models obtained by Gasbor algorithm. Left and right panels are related by 180º rotation around X-axis.

(A)

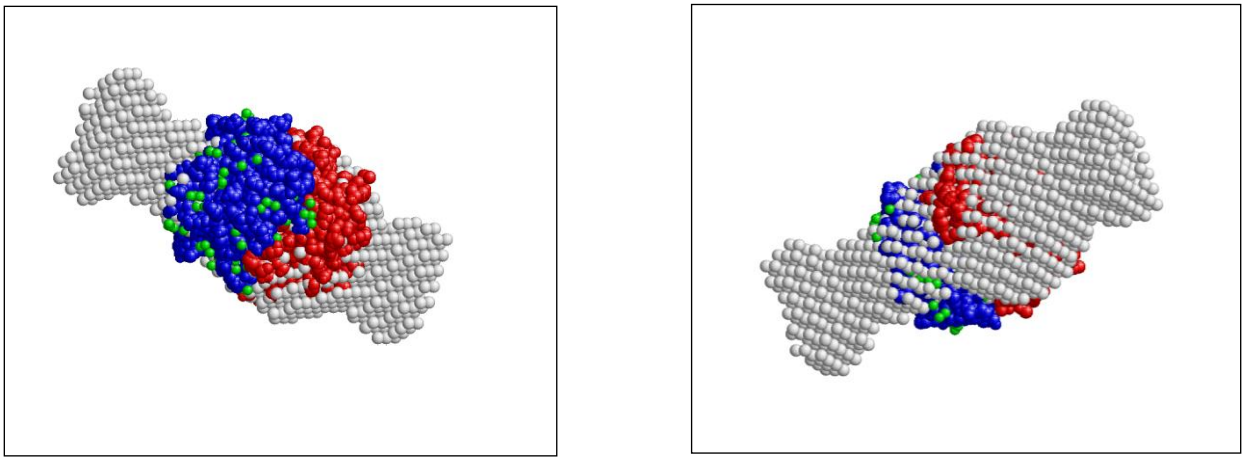

(B)

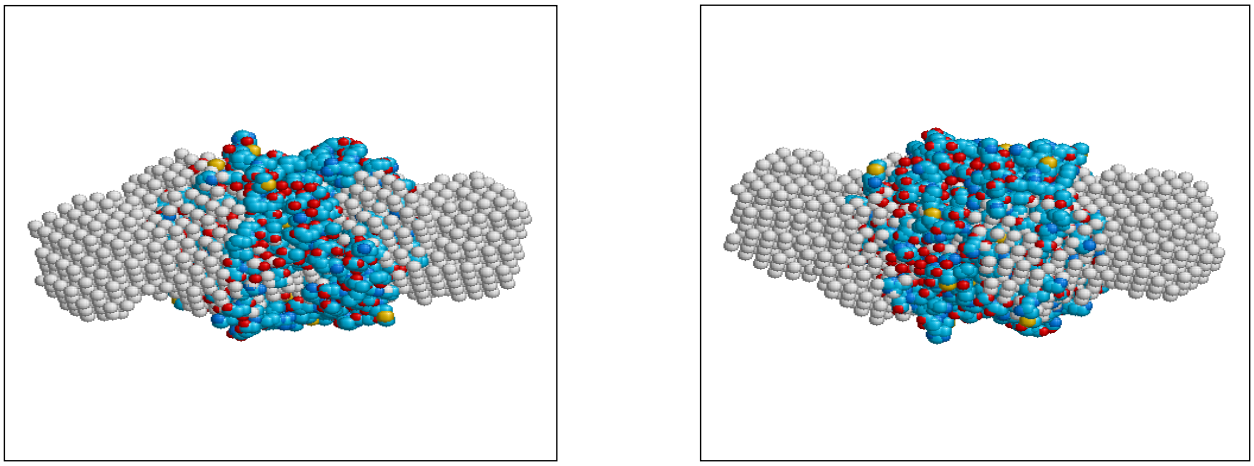

Figure 4.23: GST dimer superimposed on the shape models of G61C. (A) Models obtainded by Dammin algorithm. (B) Model obtained by Gasbor algorithm. Left and right panels are related by 180º rotation around X-axis. G61C mutant is shown in gray and GST dimer obtained from 1GTA entry is shown as yellow, red and blue.

5. DISCUSSION

More than 5 decades after the discovery of the first plant MT, the exacts functions of plant MTs are still unknown. Durum MT is a type-1 plant MT and displays three sequence domains: metal binding – Cys rich N terminus (1-19th residues) and C terminus (61-75th residues) and a long hinge region (20-60th residues).

The main aim of the present study is introduction of mutations into the cys-x-cys motifs in the alpha- and beta-domains of GSTdMT in accordance with a pattern observed in the alpha domain of vertebrate MTs to determine the effect of mutations on the Cd-binding properties and structural features of the durum MT.

5.1. Cloning, Expression, Purification and Biophysical Characterization of GSTdMT mutants

Site directed mutagenesis aimed at changing G8 and G12 in the beta domain and G61 and G65 in the alpha domain to Cys. Mutations were conducted either individually or in pairs. Single mutations gave positive results; the constructs were stable and expessed proteins were readily detected. The double mutation G61CG65C did give a mutated construct which could be sequenced but the protein could not be detected. With the double mutation G8CG12C however, it has not been possible to obtain the mutated construct at all. One reason for this result may be the low probability of annealing of the primer, with the two mismatches very close to each other in the sequence, to the template. The other possibility is that the PCR product may be at such low quantities that the linear DNA may get degraded before the circularization process in the bacteria takes place according to SDM scheme given in Appendix B.

Plant MTs are sensitive to oxidation and their long hinge region is a target for proteolytic cleavage (Tommey, *et al*., 1991). However, recombinant expression of plant MTs in bacterial systems overcomes many problems associated with direct isolation. Characterizations of nine different plant MT proteins were performed until now and eight of them were expressed as recombinant proteins in *Escherichia coli*. E_c-1 from *Triticum aestivum* is the only plant MT that has been isolated from its natural source (Hanley-Bowdoin & Lane, 1983).

Fusion partners, e.g. GST, facilitates purification, quantification, and detection. The thrombin cleavage site serves as a flexible linker between GST domain and the fused target protein domains (Zhan *et al*., 2001). This allows GST to retain its native structure and to have little interference with the structure of fused proteins (Zhan *et al*., 2001; Collak, 2009). However, GST is prone to dimerization and aggregation (Schrodel & de Marco, 2005).

dMT cDNA sequence was cloned as C-terminal fusions to GST using the pGEX-4T-2 vector. Protease deficient BL21(DE3) bacterial cells were used for overexpression of the protein (Bilecen *et al*., 2005). Other examples include the work of Murphy *et al*., 1997 on *Arabidopsis* MT1, MT2, and MT3 proteins, Abdullah *et al*., 2002 on Type III MT3-A from oil palm, Domenech et al., 2007, on Type II *Quercus suber* MT. More recently, intein tags (protein self splicing elements) were also used for recombinant expression of an Ec Type MT from *Triticum aestivum*, Type III MT from *Musa acuminata* and Type I MT from *Cicer arietinum.* (Peroza & Freisinger, 2007; Freisinger, 2007; Schicht & Freisinger, 2009).

The N- and C- terminal domains of plant MTs are protected by the formation of metal thiolate clusters, however proteolytic cleavage from the longe hinge region is still an unresolved problem (Kille et al., 1991). Hence, in the present work, 0.1 mM $CdCl_2$ was included in the growth medium to facilitate folding and stabilization.

Metals were also added during bacterial expression of other metallothioneins. For instance, during the expression of *Triticum aestivum* Ec-1 MT, 0.1 mM $ZnCl_2$ or $CdCl_2$ were used in growth media (Freisinger, 2007). For the expression of holo *Quercus suber* MT (QsMT) 0.5 mM $CuSO_4$ or 0.3 mM $ZnCl_2$ was used (Domenech et al., 2007). 0.4 mM $CdCl_2$ and $ZnCl_2$ were used during the growth of bacterial cells expressing *C. arietinum* MT1 (Schicht & Freisinger, 2009).

GSTdMT mutants were purified in two steps: Affinity chromatography and size exclusion chromatography, respectively. Affinity chromatography of GSTdMT mutants resulted in one peak with an eluate volume around 5 ml (Figure 4.8 A, B, C, and D). Protein yields of the mutants ranged between 10 to 15 mg per liter of bacterial culture. GSTdMT mutants were further purified by size exclusion chromatography. It resulted in two peaks for all mutants (Figure 4.9 A, B, C, and D). The total yield was around 20 mg from 2.25 liter of bacterial culture. The elution volume for the GST-fused mutants from the SEC corresponded to the molecular mass of the dimer protein. This result was expected since GST is known to dimerize in solution (Zhan *et al*., 2001). The SAXS results discussed below not only confirm the dimeric state of the protein but also the derived models are consistent with shapes where dMT extensions do not interact with each other.

According to results of SDS-PAGE analysis G8C and G61C mutants appear to be more prone to degradation (Figure 4.10 A, B, C and D). Which may be associated with less metal binding affinity in these proteins when compared to other mutants. Interestingly, the G65C mutant appears as a double band on SDS-PAGE. A possible explanation for this observation is given below when the metal binding properties of the mutants are discussed.

According to DLS and Native-PAGE analysis all mutants formed higher order oligomers besides dimers. These were more readily detected by Native gel analysis compared to DLS. DLS measurements of all mutants gave a main peak centered around 10 nm in the intensity distribution for the major species in solution (Figure 4.15 A, B, C and D). This corresponds to the hydrodynamic radius of expected from a protein of about 70 kDa molecular mass.

The Cd contents of the mutants as shown in Table 4.2 are 3.61±0.36 for G8C, 3.46±0.45 for G12C, 3.54±0.61 for G61C, and 4.36±0.45 for G65C; when 0.1 mM Cd was included in the growth medium of the expression cultures and in the lysis buffer. It is seen that Cd^{2+} binding enhanced by the addition of cys at the position 65. This mutation introduces a cys-cys motif at the beginning of the alpha domain of dMT. The mammalian proteins MT1 through MT3 contain three cys-cys motifs in their alpha domain and this motif is not observed in their beta domain. In these MTs alpha domain binds four metals as compared to three metals bound by the beta domain. In the case of dMT it also appears that introduction of a cys-cys motif into the alpha domain increases the likelyhood of coordinating 1 more metal

compared to the native structure. This result was obtained with several fractions from different preps. When the statistical spread is considered however, there is some overlap in the above numbers. It may be that the coordination of the additional metal is not very stable; a single cys-cys motif may not be sufficient. This may also explain the double band observed on SDS gels. The two bands may represent dMT species with different Cd content.

The charge transfer band at 250 nm observed in UV-vis absorption spectra of MTs is an indicator of Cd-S interaction (Freisinger, 2007; Willner *et al*., 1987). As can be seen in figure 4.14 B, this band is stronger with the G65C mutant confirming its higher Cd content.

5.2. Structural Analysis of GSTdMT mutants

G61C mutant was the first one obtained in significant quantities and more through analyses were carried out on this mutant. CD spectroscopic features of G61C mutant (Figure 4.18) shows the lack of strong secondary structural elements in this protein. This is in agreement with that observed from native dMT (Yesilirmak, 2008) and also with *C. arietinum* MT1 (Schicht & Freisinger, 2008). Due to time constraints CD analysis of the other mutants could not be carried out. Similarly, SAXS measurements were carried out only on G61C mutant. Shape models obtained from SAXS data of G61C indicated that the shape envelope of this mutant is similar to that of the native GSTdMT.

Having determined that G65C mutant has higher Cd content limited trypsinolysis was carried out to obtain hints about its structural features. Results indicate that the structure of G65C mutant is indeed different from the others. The slower cleavage of dMT during the experiment points to a more compact structure for the protein. It is likely that compaction is achieved in the folding of the hinge region since the major cleavage sites are there (Figure 4.12). It appears that the hinge regions of the G65C mutant is less accessible to the enzyme than that of the other mutants and hence the protein has a more compact structure.

It is reported that *C. arietinum* MT 1 may bind four or five Cd^{2+} ions and it is proposed that the structure changes according to the amount of bound metal ions. In the proposed models, binding of four divalent metal ions can be achieved in two separate clusters, whereas coordination of a fifth metal ion would require the gathering into a single joint cluster based on stoichiometric considerations (Schicht & Freisinger, 2008). However, direct experimental

proof for this model is still lacking. The G65C mutant may fold into a single metal cluster similar to *C. arietinum* MT 1. However, an alternative explanation may be dimerization may involve not only the GST molecules but dMT extensions may also be positioned against each other to accommodate more metals.

6. CONCLUSIONS AND FUTURE WORK

The work presented in this thesis concerns the expression, purification, and biochemical and biophysical characterization of mutant GSTdMT constructs to gain insight into the structural and functional properties of the native protein. The basic conclusions from this work can be summarized as follows:

- The distribution of cys-x-cys motifs and interspaced residues in the dMT sequence is such that mutations involving a single amino acid to generate a cys-cys motif can be more easily achieved than those generating two consequtive cys-cys motifs in the same domain.
- Of the four mutants, only one (the G65C mutant) showed enhanced Cd binding with a ratio of 4.36±0.45 Cd^{2+} per protein, thus binding an additional Cd for each mole of protein compared to native GSTdMT.
- G65C binds Cd^{2+} more tightly, since the charge transfer band of G65C seems to be stronger compared to G8C, G12C and G61C mutants.
- Evidence from the proteolytic degradation experiments indicates that G65C has more compact structure.
- Same as native dMT, G61C mutant is mostly composed of random coils.
- Shape models obtained from SAXS data of G61C indicated that the shape envelope of this mutant is similar to that of the native GSTdMT.

G65C mutant promises to be a good candidate for different applications including development of metal biosensors or for environmental applicaitons. Additional work is needed to understand if G65C retains its enhanced metal binding capacity also when it is cleaved from GST. Further structural work would provide insights into metal binding mechanism of this protein and show its features that are different from native dMT. Work is

also needed to understand domain specificity of mutations and their implications on metal binding.

7. REFERENCES

1. Abdullah, S. N. A., Cheah, S. C., Denis, J. M. (2002). Isolation and characterization of two divergent type 3 metallothioneins from oil palm, *Elaeis guineensis. Plant Physiology and Biochemistry*, 40(3),255-263.
2. Ambler, J., Rodgers, M. (1980). Two new non-barbituratw buffers for electrophoresis of serum proteins on cellulose acetate membranes. *Clinical Chemistry*, 26(8), 1221-1223.
3. Andrews, G.K. (2000) Regulation of metallothionein gene expression by oxidative stres and metal ions. *Biochemical Pharmacology* 59, 95-104.
4. Bilecen, K., Ozturk, U. H., Duru, A. D., Sutlu, T., Petoukhov, M. V., Svergun, D. I., Koch, M. H., Sezerman, U. O., Cakmak, I., Sayers, Z. (2005). Triticum durum metallothionein. Isolation of the gene and structural characterization of the protein using solution scattering and molecular modeling. *Journal of Biological Chemistry*, 280(14), 13701-11.
5. Binz, P. A., Kagi, J. H. R. (1999). Metallothionein: Molecular evolution and classification in: C. Klaassen (Ed.), Metallothionein IV, Birkhauser Verlag, Basel, p.7.
6. Braun, W., Vasak, M., Robbins, A. H., Stout, C. D., Wagner, G., Kagi, J. H. R., Wüthrich, K. (1992). Comparison of the NMR solution structure and the x-ray crystal structure of rat metallothionein-2. *Proceedings of the National Academy of Sciences USA*, 89, 10124-10128.
7. Briat, J. F., Lebrun, M. (1998). Plant responses to metal toxicity. *Plant biology and pathology*, 322, 43-54.

8. Cobbett, C., Goldsbrough, P. (2002). Phytochelatins and metallothioneins: Roles in heavy metal detoxification and homeostasis. *Annual Review of Plant Biology*, 53, 159-82.
9. Collak, F. K. (2009). Cloning, expression, and purification of durum wheat metallothionein domains and structural modelling. Ph. D. Thesis, Sabanci University.
10. Dallinger, R., Berger, B., Hunziker, P., Kagi, J. H. (1997). Metallothionein in snail Cd and Cu metabolism. *Nature*, 388, 237-238.
11. Domenech, J., Orihuela, R., Mir, G., Molinas, M., Atrian, S., Capdevila, M. (2007). The Cd(II)-binding abilities of recombinant Quercus suber metallothionein: bridging the gap between phytochelatins and metallothioneins. *Journal of Inorganic Biochemistry*, 12(6), 867-82.
12. Fontana, A., Laureto, P. P., Spolaore, B., Frare, E., Picotti, P., Zambonin, M. (2004). Probing protein structure by limited proteolysis. *Acta Biochimica Polonica*, 52(2), 299-321.
13. Freisinger, E. (2008). Plant MTs-long neglected members of the metallothionein superfamily. *Dalton Transactions*, 47, 6649-6852.
14. Fürst, P., Hu, S., Hackett, R., Hamer, D. (1988). Copper activates metallothionein gene transcription by altering the conformation of a specific DNA binding protein. *Cell*, 55(4), 705-17.
15. Guinier, A., Fournet, G. (1955). Small Angle Scattering of X-rays, John Wiler, New York, 19-23.
16. Guo, W. J., Bundithya, W., Goldsbrough, P. B. (2003). Characterization of the Arabidopsis metallothionein gene family: tissue-specific expression and induction during senescence and in response to copper. *New Phytologist*, 159, 369-381.
17. Hanley-Bowdoin, L., Lane, B. G. (1983). A novel protein programmed by the mRNA conserved in dry wheat embryos. The principal site of cysteine incorporation during early germination. *European Journal of Biochemistry*, 135(1), 9-15.
18. Hsieh, H. M., Liu, W. K., Huang, P. C. (1995). A novel stress-inducible metallothionein-like gene from rice. *Plant Molecular Biology*, 28(3), 381-9.
19. Hsieh, H. M., Liu, W. K., Chang, A., Huang, P. C. (1996). RNA expression patterns of a type 2 metallothionein-like gene from rice. *Plant Molecular Biology*, 32(3), 525-9.
20. Kagi, J. H., Schaffer, A. (1988). Biochemistry of metallothionein. *Biochemistry*, 27(23), 8509-15.

21. Kagi, J. H. R., Riordan, J. F., Vallee, B. L. (1991). Overview of Metallothionein. *Methods in Enzymology*, 205, 613-626.
22. Karin, M., Haslinger, A., Holtgreve, H., Cathala, G., Slater, E., Baxter, J. D. (1984). Activation of a heterologous promoter in response to dexamethasone and cadmium by metallothionein gene 5'-flanking DNA. *Cell*, 36(2), 371-9.
23. Kille, P., Winge, D. R., Harwood, J. L., Kay, J. (1991). A plant metallothionein produced in *E. coli*. *FEBS Letters*, 295, 171-175.
24. Klaasen, C. D. (ed.) (1999) MetallothioneinsIV, Birkhauser Verlag, Basel.
25. Koch, M. H. J., Bordas, J. (1983). X-ray diffraction and scattering on disordered systems using synchrotron radiation. *Nuclear Instruments and Methods*, 208, 461-469.
26. Kojima, Y., Binz, P. A., Kagi, J. H. R. (1999). Nomenclature of metallothionein: proposal for a revision, in: C. Klaassen (Ed.), Metallothionein IV, Birkhauser Verlag, Basel, p.3.
27. Konarev, P. V., Volkov, V. V., Sokolova, A. V., Koch M. H. J., Svergun, D. I. (2003). PRIMUS: a Windows PC-based system for small-angle scattering data analysis. *Journal of Applied Crystallography* 36, 1277-1282.
28. Laemmli, U. K. (1970). Cleavage of structural proteins during the assembly of the head of bacteriophage T4. *Nature*, 227(5259), 680-685.
29. Maret, W. (2009). Fluorescent probes for the structure and function of metallothionein. *Journal of Chromatography B*, 877, 3378-3383.
30. Margoshes, M., Vallee, B. L. (1957). A cadmium protein from equine kidney cortex. *Journal of the American Chemical Society*, 79, 4813-4814.
31. Murphy, A., Zhou, J., Goldsbrough, P. B., Taiz, L. (1997). Purification and immunological identification of metallothioneins 1 and 2 from *Arabidopsis thaliana*. *Plant Physiology*, 113, 1293-1301.
32. Olafson, R. W., McCubbin, W. D., Kay, C. M. (1988). Primary- and secondary-structural analysis of a unique prokaryotic metallothionein from a Synechococcus sp. Cyanobacterium. *Biochemical Journal*, 215(3), 691-9.
33. Peroza, E. A., Freisinger, E. (2007). Metal ion binding properties of Triticum aestivum Ec-1 metallothionein: evidence supporting two separate metal thiolate clusters. *Journal of Biological Inorganic Chemistry*, 12, 377-391.
34. Peroza, E. A., Kaabi, A. A., Meyer-Klaucke, W., Wellenreuther, G., Freisinger, E. (2008). The two distinctive metal ion binding domains of the wheat metallothionein Ec-1. *Journal of Inorganic Biochemistry*, 103(3), 342-353.

35. Peroza, E. A., Schmucki, R., Güntert, P., Freisinger, E., Zerbe, O. (2009). The βE-domain of wheat Ec-1 metallothionein: A metal-binding domain with a distinctive structure. *Journal of Molecular Biology*, 387, 207-218.
36. Petoukhov, M. V., Konarev, P., Kikhney, A. G., Svergun, D. I. (2007). *ATSAS* 2.1 - towards automated and web-supported small-angle scattering data analysis. *Journal of Applied Crystallography* 40 (Supplement), 223-228.
37. Porod, G. (1982). General Theory, in: O. Glatter, O. Kratky (Eds.) Small-angle X-ray Scattering. *Academic Press*, 17-51.
38. Pulido, P., Kagi, J. H. R., Vallee, B. L. (1960). Isolation and some properties of human metallothionein. *Biochemistry*, 5(5), 1768-1777.
39. Quaife, C. J., Findley, S.D., Erickson, J. C., Froelick, G. J., Kelly, E. J., Zambrowics, B. P., Palmiter, R. D. (1994). Induction of a new metallothionein isoform (MT-IV) occurs during differentiation of stratified squamous epithelia. *Biochemistry*, 33, 7250-7259.
40. Rauser, W. E. (1999). Structure and function of metal chelators produced by plants: the case for organic acids, amino acids, phytin, and metallothioneins. *Cell Biochemistry and Biophysics*, 31(1), 19-48.
41. Rigby, K. E., Stillman, M. J. (2004) Structural studies of metal-free metallothionein. *Biochemical and Biophysical Research Communications*, 325, 1271-1278.
42. Robbins, A. H., McRee, D. E., Williamson, M., Collett, S. A., Xuong, N. H., Furey, W. F., Wang, B. C., Stout, C. D. (1991). Refined crystal structure of Cd, Zn metallothionein at 2.0 A resolution. *Journal of Molecular Biology*, 221, 1269-1293.
43. Robinson, N. J., Tommey, A. M., Kuske, C., Jackson, P. J. (1993). Plant metallothioneins. *Biochemical Journal*, 295, 1-10.
44. Roessle, M. W., Klaering, R., Ristau, U., Robrahn, B., Jahn, D., Gehrmann, T., Konarev, P., Round, A., Fiedler, S., Hermes, C. & Svergun, D.I. (2007) Upgrade of the small-angle X-ray scattering beamline X33 at the European Molecular Biology Laboratory, Hamburg. *Journal of Applied Crystallography* 40, 190-194.
45. Romero-Isart, N., Oliva, B., Vasak, M. (2010) Influence of NH-SH bonding interactions on the structure and dynamics of metallothioneins. *Journal of Molecular Modeling* 16, 387-394.
46. Sambrook, J., Manniatis, T., Fritsh, E. F. (1989). Molecular Cloning: A Laboratory Manual. Cold Spring Harbor Laboratory Press. 2nd Edition.

47. Schicht, O., Freisinger, E. (2008). Spectroscopic characterization of *Cicer arietinum* metallothionein 1. *Inorganica Chimica Acta*, 362(3), 714-724.
48. Schrodel, A., de Marco, A. (2005). Characterization of the aggregates formed during recombinant protein expression in bacteria. *BMC Biochemistry*, 6-10.
49. Schultze, P., Worgotter, E., Braun, W., Wagner, G., Vasak, M., Kagi, J. H. R., Wüthrich, K. (1988). Conformation of [Cd_7]-metallothionein-2 from rat liver in aqueous solution determined by nuclear magnetic resonance spectroscopy. *Journal of Molecular Biology*, 203, 251-268.
50. Svergun, D. I. (1992). Determination of the regularization parameter in indirect-transform methods using perceptual criteria. *Journal of Applied Crystallography* 25, 495-503.
51. Svergun, D. I. (1999). Restoring low resolution structure of biological macromolecules from solution scattering using simulated annealing. *Biophysical Journal*, 76, 2879-2886.
52. Svergun, D. I., Petoukhov, M. V., Koch, M. H. J. (2001). Determination of domain structure of proteins from X-Ray solution scattering. *Biophysical Journal*, 80, 2946-2953.
53. Svergun, D. I., Koch, M. H. J. (2002). Advances in structure analysis using small-angle scattering in solution. *Current Opinion in Structural Biology*, 12, 654-660.
54. Svergun, D. I., Koch, M. H. J. (2003). Small-angle scattering studies of biological macromolecules in solution. *Reports on Progress in Physics*, 66, 1735-1782.
55. Tommey, A. M., Shi, J., Lindsay, W. P., Urwin, P. E., Robinson, N. J. (1991). Expression of the pea gene PSMTA in *E. coli*. Metal-binding properties of the expressed protein. *FEBS Letters*, 291(1-2), 48-52.
56. Vallee, B. L. (1995). The function of metallothionein. *Neurochemistry International*, 27(1), 23-33.
57. Vasak, M., Kagi, J. H. R. (1994). Metallothioneins. *Encyclopedia of Inorganic Chemistry*, 4, 2229-2241.
58. Vasak, M., Hasler, D. W. (2000). Metallothioneins: New functional and structural insights. *Current Opinion in Chemical Biology*, 4, 177-183.
59. Vasak, M., Romero-Isart, N. (2002). Advances in the structure and chemistry of metallothioneins. *Journal of Inorganic Biochemistry*, 88, 388-396.
60. Vasak, M. (2005). Advances in metallothionein structure and functions. *Journal of trace elements in medicine and biology*, 19, 13-17.

61. Vasak, M., Romero-Isart, N. Metallothioneins. (2005). In: King RB (ed.), *Encyclopedia of Inorganic Chemistry*, 2nd ed, 3208-3221.
62. Volkov, V. V., Svergun, D. I. (2003). Uniqueness of ab initio shape determination in small-angle scattering**.** *Journal of Applied Crystallography*, 36, 860-864.
63. Willner, H., Vasak, M., Kagi, J. H. R. (1987). Cadmium-thiolate clusters in metallothionein: Spectrophotometric and spectropolarimetric features. *Biochemistry*, 26, 6287-6292.
64. Yesilirmak, F. (2008). Biophysical and functional characterization of wheat metallothionein at molecular level. Ph.D. Thesis, Sabanci University.
65. Zhan, Y., Song, X., Zhou, G. W. (2001). Structural analysis of regulatory protein domains using GST-fusion proteins. *Gene*, 281(1-2), 1-9.
66. Zhou, J., Goldbrough, B. B. (1994). Functional homologs of fungal metallothionein genes from Arabidopsis. *Plant Cell*, 6(6), 875-84
67. Zhou, J., Goldbrough, B. B. (1995). Structure, organization and expression of the metallothionein gene family in Arabidopsis. *Molecular and General Genetics*, 248(3), 318-28.

APPENDIX A

CHEMICALS

Acetic acid (glacial)	Riedel-de Haen, Germany	27225
30 % Acrylamide-0.8 % Bisacrylamide	Sigma, Germany	A3699
Bromophenol blue	Applichem, Germany	A3640
Cadmium (II) sulphate	Fluka, Switzerland	20920
Coomassie Brillant Blue R-250	Fluka, Switzerland	27816
Complete Protease Inhibitor Cocktail Tablets	Roche	11 836 145 001
dNTP mix	Fermentas, Germany	R0241
1,4-Dithiothreitol	Fluka, Switzerland	43815
*Eco*RI	Fermentas, Germany	ER0271
Ethanol	Riedel-de Haen, Germany	32221
Ethylenediaminetetraaceticacid	Riedel-de Haen, Germany	27248
Glycerol (87 %)	Riedel-de Haen, Germany	15523
Glycine	Amresco, USA	0167
HEPES	Fluka	54461
Hydrochloric acid (37 %)	Merck, Germany	100314
IPTG	Fermentas, Germany	R0392
MassRuler DNA Ladder Mix	Fermentas, Germany	SM0403
2-Mercaptoethanol	Aldrich, Germany	M370-1
Methanol	Riedel-de Haen, Germany	24229
PageRuler protein ladder	Fermentas, Germany	SM0661
Phenylmethylsulphonylfluoride	Amresco, USA	0754
2-Propanol	Merck, Germany	100996

Protein Molecular Weight Marker	Fermentas, Germany	SM0431
Reduced Glutathione	Merck, Germany	K33271590522
Silver staining plus kit	BioRad	161-0449
Site-Directed Mutagenesis Kit	Stratagene	200518
Sodium Chloride	Riedel-de Haen, Germany	13423
Sodium dodecyl sulphate	Sigma, Germany	L-4390
Taq polymerase	Fermentas, Germany	EP0401
Thrombin	GE-Healthcare, Sweden	27-0846-01
Tris	Fluka, Switzerland	93349
Triton X-100	Applichem, Germany	A1388
Unstained protein MW marker	Fermentas, Germany	SM0431
*Xho*I	Fermentas, Germany	ER0691

MOLECULAR WEIGHT MARKERS

MassRuler DNA Ladder Mix

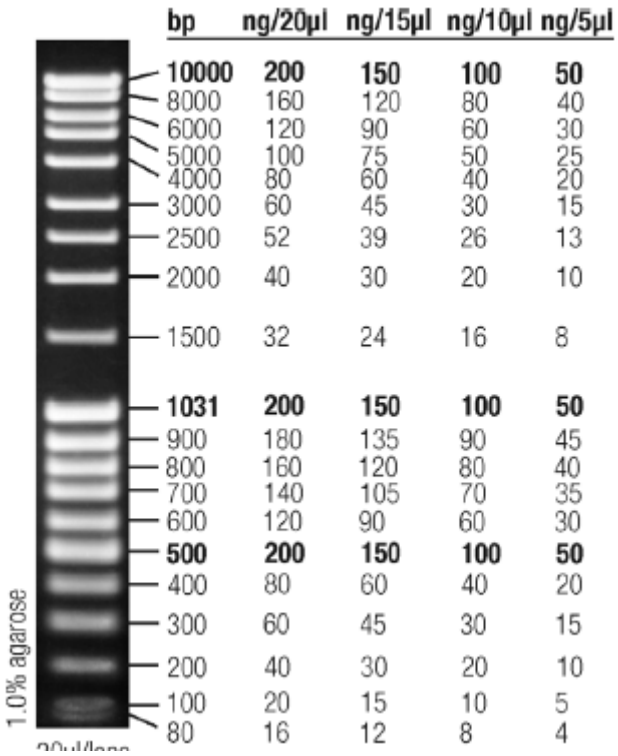

bp	ng/20µl	ng/15µl	ng/10µl	ng/5µl
10000	**200**	**150**	**100**	**50**
8000	160	120	80	40
6000	120	90	60	30
5000	100	75	50	25
4000	80	60	40	20
3000	60	45	30	15
2500	52	39	26	13
2000	40	30	20	10
1500	32	24	16	8
1031	**200**	**150**	**100**	**50**
900	180	135	90	45
800	160	120	80	40
700	140	105	70	35
600	120	90	60	30
500	**200**	**150**	**100**	**50**
400	80	60	40	20
300	60	45	30	15
200	40	30	20	10
100	20	15	10	5
80	16	12	8	4

Unstained protein MW marker

MW, kDa	Protein	Source	Ref.
116.0	β–galactosidase	*E.coli*	2
66.2	Bovine serum albumin	bovine plasma	3
45.0	Ovalbumin	chicken egg white	4
35.0	Lactate dehydrogenase	porcine muscle	5
25.0	REase Bsp98I	*E.coli*	6
18.4	β–lactoglobulin	bovine milk	7
14.4	Lysozyme	chicken egg white	8

12% Tris-glycine SDS-PAGE

APPENDIX B

pGEX-4T-2 vector map and multicloning site with available restriction enzyme sites

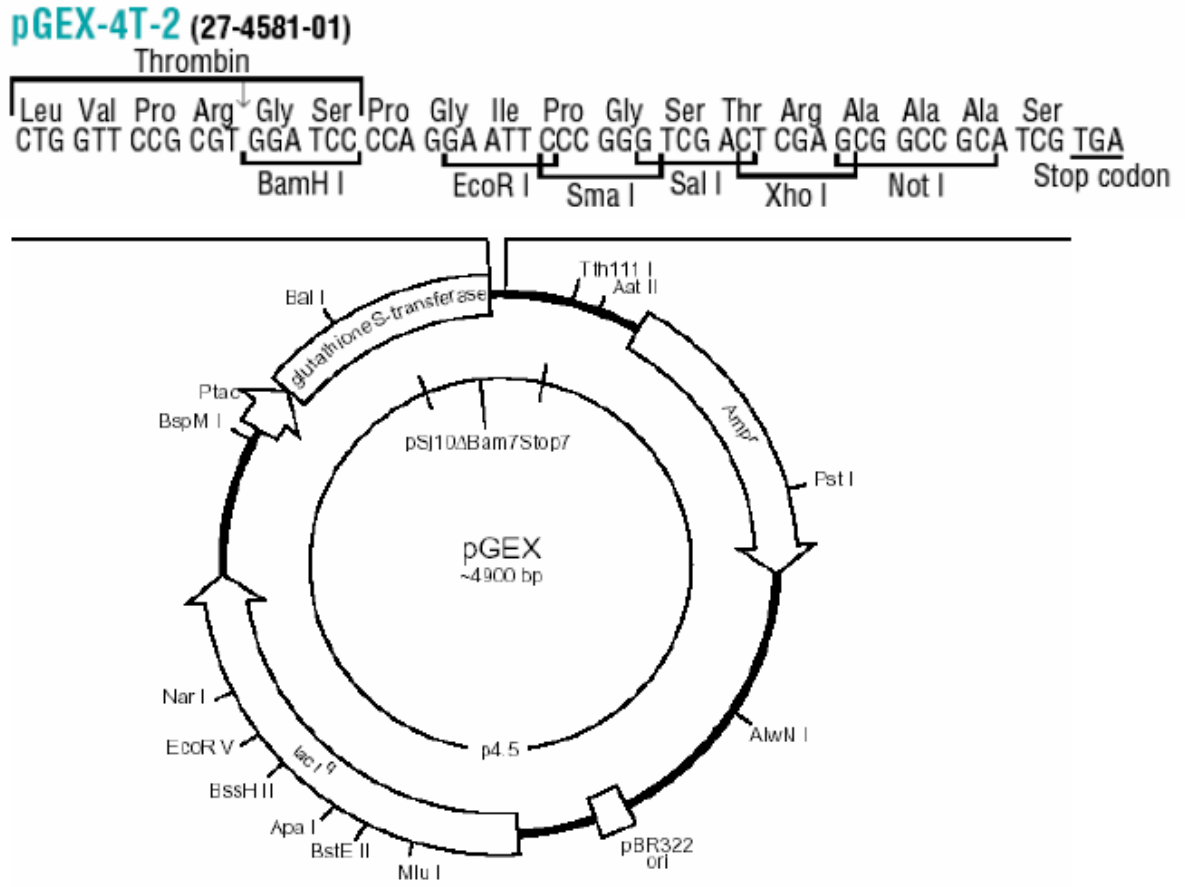

Overview of the Site-Directed Mutagenesis Method

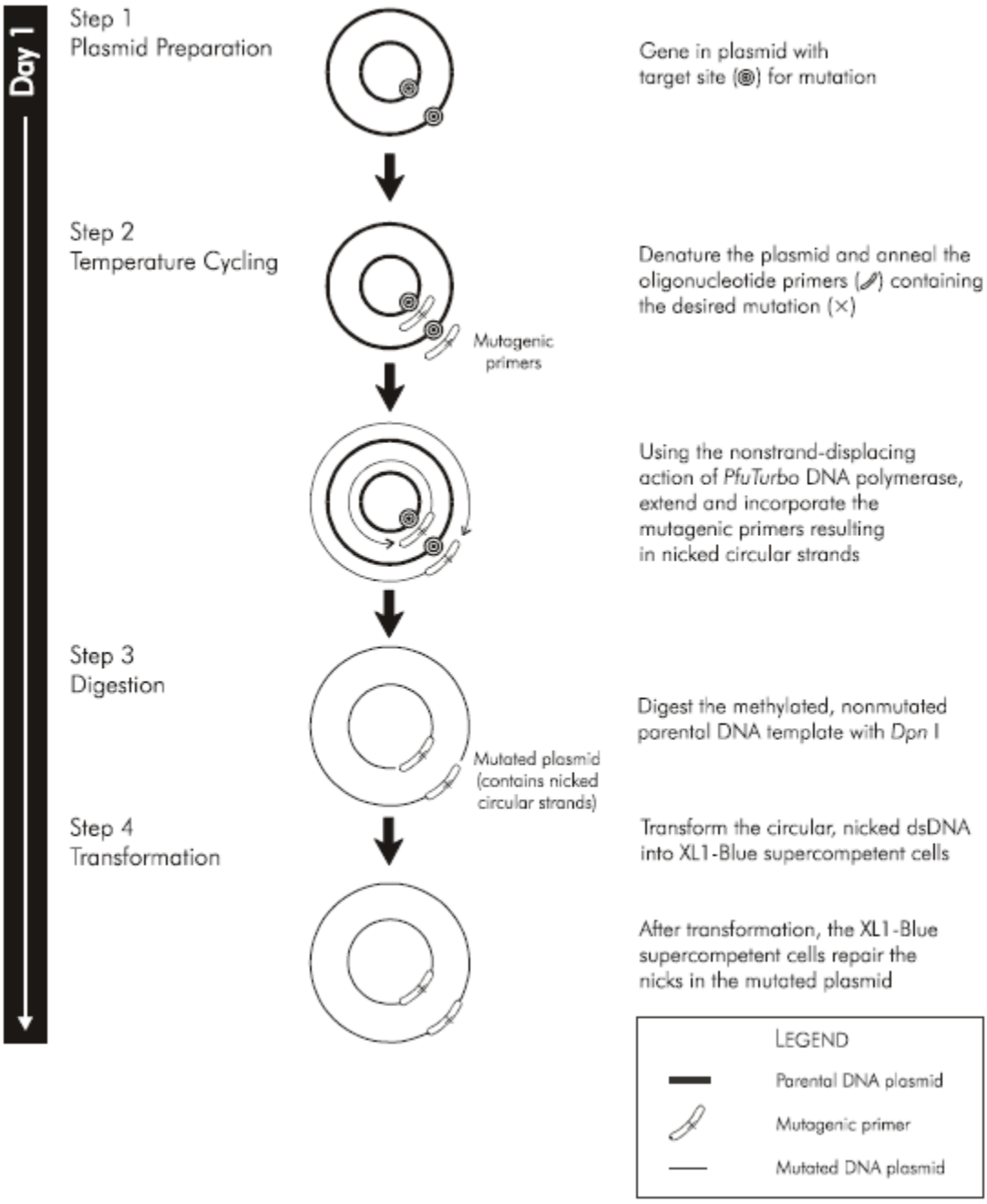

Sequencing Results of GSTdMT Mutants

```
                 190        200        210
dMTgene  GGCTGCAGCTGCGGCGACAACTGCAAGTGCAA
         :::::::::::: ::::::::::::::::::
G6165C   TGCTGCAGCTGCTGCGACAACTGCAAGTGCAA
         240        250        260        270

                  10         20         30
dMTgene  ATGTCTTGCAACTGTGGATCCGGTTGCAGCTG
         :::::::::::::::::::: ::::::::::
G8C      ATGTCTTGCAACTGTGGATCCTGTTGCAGCTG
            60         70         80

                   30         40         50
dMTgene  CCGGTTGCAGCTGCGGCTCAGACTGCAAGTG
         :::::::::::::: ::::::::::::::::
G12C     CCGGTTGCAGCTGCTGCTCAGACTGCAAGTG
             80         90        100

         181    190        200
dMTgene  GGCTGCAGCTGCGGCGACAACTGCAAGTGCGAG
         ::::: :::::::::::::::::::::::::::
G61C     TGCTGCCGCTGCGGCGACAACTGCAAGTGCGAG
           240        250        260

                 190        200        210
dMTgene  GGCTGCAGCTGCGGCGACAACTGCAAGTGCAA
         :::::::::::: ::::::::::::::::::
G65C     GGCTGCAGCTGCTGCGACAACTGCAAGTGCAA
         240        250        260        270
```

APPENDIX C

BUFFERS AND SOLUTIONS

Tris Acetate EDTA Buffer (TAE) (50X): 121.1 g Tris Base, 28.55 ml Glacial Acetic acid, 7.3 g EDTA, completed to 500 ml.

Native-PAGE:

8% Separating Gel:

	for 2 gels	for 1 gel	[final]
dH_2O	6 ml	3 ml	
3 M Tris, pH 8.9	1.25 ml	625 µl	3.75 mM
30 % Acryl-0.8 % Bisacryl	2.67 ml	1.335 ml	8 %
10 % APS	75 µl	37.5 µl	0.075 %
TEMED	5 µl	2.5 µl	0.05 %

3 % Stacking Gel:

	for 2 gels	for 1 gel	[final]
dH_2O	4.2 ml	2.1 ml	
1 M Tris, pH 6.8	250 µl	125 µl	50 mM
30 % Acryl-0.8 % Bisacryl	510 µl	255 µl	3 %
10 % APS	37.5 µl	18.75 µl	0.075 %
TEMED	2.5 µl	1.25 µl	0.05 %

2X Native Sample Buffer: 200 mM Tris-HCl pH 7.5, 20 % (v/v) Glycerol, 0.05 % (w/v) Bromophenol Blue in ddH_2O.

Native-PAGE Running Buffer: 25 mM Tris, 192 mM Glycine in ddH_2O.

SDS-PAGE:

12 % Separating Gel:

	for 2 gels	for 1 gel	[final]
dH_2O	4.62 ml	2.31 ml	
3 M Tris, pH 8.9	1.25 ml	625µl	3.75 mM
30 % Acryl-0.8 % Bisacryl	4 ml	2 ml	12 %
20 % SDS	50 µl	25 µl	0.1 %
10 % APS	75 µl	37.5µl	0.075 %
TEMED	5 µl	2.5 µl	0.05 %

5 % Stacking Gel:

	for 2 gels	for 1 gel	[final]
dH_2O	3.850 ml	1.925 ml	
3 M Tris, pH 8.9	250 µl	125 µl	50 mM
30 % Acryl-0.8 % Bisacryl	850 µl	425µl	5 %
20 % SDS	10 µl	5 µl	0.1 %
10 % APS	37.5 µl	18.75 µl	0.075 %
TEMED	2.5 µl	1.25µl	0.05 %

2X SDS Sample Buffer: 4 % (w/v) SDS, 20 % (v/v) Glycerol, 0.004 % (w/v) Bromophenol blue, 10 % (v/v) 2-mercaptoethanol, 0.125 M Tris-HCl, pH 6.8 in ddH_2O.

SDS-PAGE Running Buffer: 25 mM Tris, 192 mM Glycine, 0.1 % (w/v) SDS in ddH_2O.

Tris-Tricine Gel:

	16 % Resolving Gel	3 % Stacking Gel
29:1 Acrylamide/bisacrylamide	2.5 ml	400 µl
Tris-Cl/SDS, pH 8.45	2.5 ml	1.24 ml
Glycerol	1 ml	-
TEMED	5 µl	4 µl
10 % APS	60 µl	40 µl
dH_2O	1.4 ml	3.3 ml

Tris-Tricine Gel Running Buffers:

1X Cathode Buffer (Load on top into wells): 0.1 M Tris, 0.1 M Tricine, and 0.1 % SDS in ddH_2O.

1X Anode Buffer (Load on gel apparatus tray): 0.2 M Tris-Cl, pH 8.9 in ddH_2O.

Coomassie Staining Solution: 0.1 % (w/v) Coomassie Brillant Blue R-250, 40 % (v/v) Methanol, 10 % (v/v) Glacial Acetic acid in ddH_2O.

Destaining Solution: 4 % (v/v) Methanol, 7.5 % (v/v) Glacial Acetic acid, completed to 1 L.

APPENDIX D

EQUIPMENTS

AKTA FPLC:	GE-Healthcare, SWEDEN
Autoclave:	Hirayama, Hiclave HV-110, JAPAN
	Certoclav, Table Top Autoclave CV-EL-12L, AUSTRIA
Cenrifuge:	Eppendorf, 5415C, GERMANY
	Eppendorf, 5415D, GERMANY
	Eppendorf, 5415R, GERMANY
	Hitachi, Sorvall RC5C Plus, USA
	Hitachi, Sorvall Discovery 100 SE, USA
Dynamic Light Scattering:	Malvern, Zetasizer Nano-ZS, UK
Deepfreeze:	-80 ^{o}C, Kendro Lab. Prod., Heraeus Hfu486, GERMANY
	-20 ^{o}C, Bosch, TURKEY
Distilled water:	Millipore, Elix-S, FRANCE
	Millipore, MilliQ Academic, FRANCE
Electrophoresis:	Biogen Inc., USA
	Biorad Inc., USA
Ice Machine:	Scotsman Inc., AF20, USA
ICP-OES:	Varian, Vista-Pro CCD, AUSTRALIA
Incubator:	Memmert, Modell 300, GERMANY
	Memmert, Modell 600, GERMANY

Laminar Flow:	Kendro Lab. Prod., Heraeus, HeraSafe HS12, GERMANY
Magnetic Stirrer:	VELP Scientifica, ARE Heating Magnetic Stirrer, ITALY
	VELP Scientifica, Microstirrer, ITALY
Microliter Pipette:	Gilson, Pipetman, FRANCE
Microwave Oven:	Bosch, TURKEY
pH Meter:	WTW, pH540 GLP MultiCal, GERMANY
Power Supply:	Biorad, PowerPac 300, USA
	Wealtec, Elite 300, USA
Refrigerator:	+4 ^{o}C, Bosch, TURKEY
Shaker:	Forma Scientific, Orbital Shaker 4520, USA
	GFL, Shaker 3011, USA
	New Brunswick Sci., Innova 4330, USA
Sonicator:	BioBlock Scientific, Vibracell 7504, FRANCE
Spectrophotometer:	Nanodrop, ND-1000, USA
Speed Vacuum:	Savant, Speed Vac Plus Sc100A, USA
	Savant, Refrigerated Vapor Trap RVT 400, USA
Thermocycler:	Eppendorf, Mastercycler Gradient, GERMANY